CR 189304

FINAL REPORT
NATIONAL SCIENCE FOUNDATION GRANT NO. ATM-9207345
NASA GODDARD SPACE FLIGHT CENTER, P.R. No. 913-44468

TEST OF PROTOTYPE LIQUID-WATER-CONTENT METER FOR AIRCRAFT USE

Submitted by:

Dr. Hermann E. Gerber
Gerber Scientific Inc.
1643 Bentana Way
Reston, VA 22090
(703-742-9844)

March 12, 1993

Submitted to:

Dr. Ronald C. Taylor, Program Director
Physical Meteorology Program
Room 644
National Science Foundation
1800 G Street, NW
Washington, D.C. 20550

Dr. Michael D. King
Laboratory for Atmospheres
NASA Goddard Space Flight Center
Greenbelt, MD 20771

FINAL REPORT
NATIONAL SCIENCE FOUNDATION GRANT NO. ATM-9207345
NASA GODDARD SPACE FLIGHT CENTER, P.R. No. 913-44468

TEST OF PROTOTYPE LIQUID-WATER-CONTENT METER FOR AIRCRAFT USE

Submitted by:

Dr. Hermann E. Gerber
Gerber Scientific Inc.
1643 Bentana Way
Reston, VA 22090
(703-742-9844)

March 12, 1993

Submitted to:

Dr. Ronald C. Taylor, Program Director
Physical Meteorology Program
Room 644
National Science Foundation
1800 G Street, NW
Washington, D.C. 20550

Dr. Michael D. King
Laboratory for Atmospheres
NASA Goddard Space Flight Center
Greenbelt, MD 20771

Table of Contents

1. INTRODUCTION

This report describes the effort undertaken to meet the objectives of National Science Foundation Grant ATM-9207345 titled "Test of Prototype Liquid-Water-Content Meter for Aircraft Use." Three activities were proposed for testing the new aircraft instrument, PVM-100A:

1) Calibrate the PVM-100A in a facility where the liquid-water-content (LWC) channel, and the integrated surface area channel (PSA) could be compared to standard means for LWC and PSA measurements. Scaling constant for the channels were to be determined in this facility. The fog/wind tunnel at ECN, Petten, The Netherlands was judged the most suitable facility for this effort.

2) Expose the PVM-100A to high wind speeds similar to those expected on research aircraft, and test the anti-icing heaters on the PVM-100A under typical icing conditions expected in atmospheric clouds. The high-speed icing tunnel at NRC, Ottawa, Canada was to be utilized.

3) Operate the PVM-100A on an aircraft during cloud penetrations to determine its stability and practicality for such measurements. The C-131A aircraft of the University of Washington was the aircraft of opportunity for these tests, which were to be conducted during the 4-week Atlantic Stratocumulus Transition Experiment (ASTEX) in June of 1992.

The operating principle and configuration of the PVM-100A is summarized as follows: This new instrument is based on the adaptation of an existing instrument, the PVM-100 (Gerber, 1991), used for ground-based measurements of LWC. The operating principle of both instruments is the same: Light scattered into the forward direction by cloud droplets is weighted as a function scattering angle by a spatial filter with variable transmission in annular regions. The filter is computer designed by inverting the integral describing the light scattering; for more detail see Gerber (1992) in Appendix A, and Gerber et al. (1993) in Appendix B. The PVM-100A differs primarily from the ground-based version in that its design reflects its intended use on aircraft. Figure 1 shows the configuration and dimensions of the PVM-100A probe. The cylindrical annulus faces into the wind during flight. Other differences include electronics fast enough to deal with the higher air speed encountered in aircraft use, and the use of two additional channels. Besides the LWC channel, the PVM-100A includes a PSA channel, and a third channel for measuring depolarized backscattered light. The capability to simultaneously measure LWC and PSA is significant, because the effective droplet radius, $r_e(um) = 30000x(LWC, g/m^3)/(PSA, cm^2/m^3)$, is an indicator of the anthropogenic effect on clouds, and is used to parameterize the radiative effects of clouds.

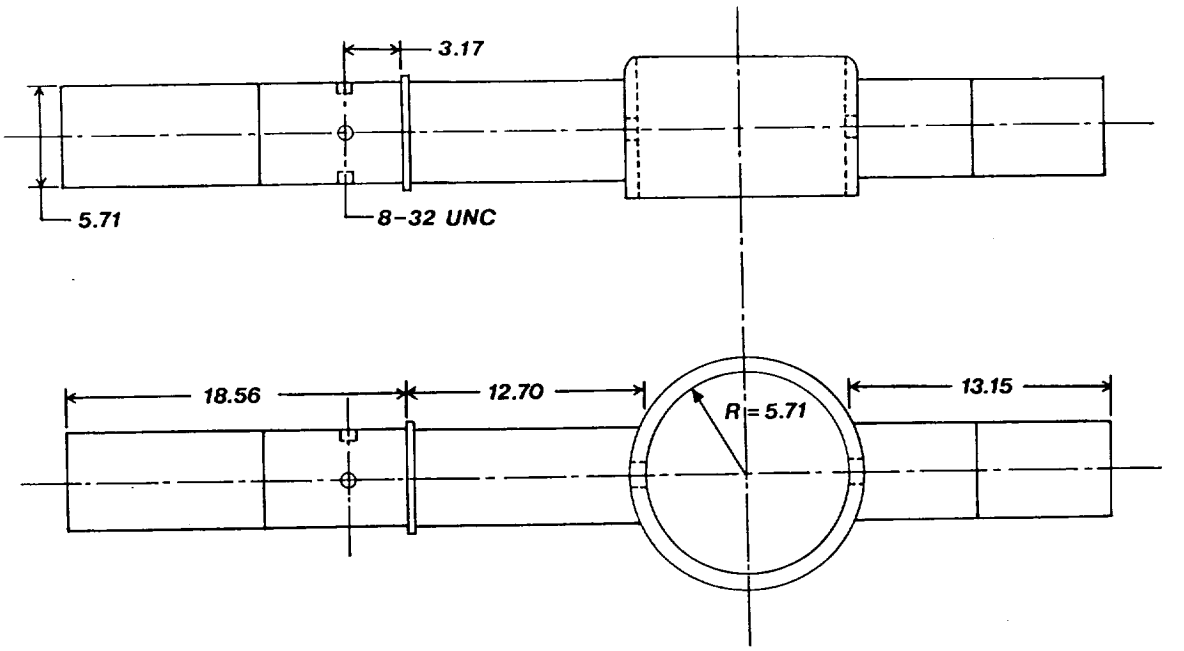

Fig. 1 - Probe of PVM-100A; top view (upper), rear view (lower). Dimensions in cm.

The development of the PVM-100A is an attempt to improve the accuracy of measuring LWC and PSA of cloud droplets and ice crystals from aircraft. Present instruments used to measure these cloud microphysical parameters include the Johnson-Williams hot-wire probe, the CSIRO (King, et al., 1978) hot-wire probe, and the FSSP-100 (Forward Scattering Spectrometer Probe; Particle Measuring Systems, Boulder, CO). The hot-wire probes have a tendency for underestimating LWC at higher aircraft speeds (Strapp and Schemenauer, 1982), and the FSSP-100 instruments differ from each other so that corrections applied to their output do not necessarily lead to accurate results (Cooper, 1988; Baumgardner and Spowart, 1990). The PVM instruments differ from the preceding approaches in that their output does not depend on rate of droplets passing through or impacting the instrument. The PVM output is designed to be independent of air speed. The cloud sample volumes of the PVM are about 50,000 larger than the sample volume in the FSSP-100. This difference and the independence from air speed permits the PVM to measure LWC more accurately. The ground-based instrument, PVM-100, was shown to have an accuracy better than 10% (Arends et al., 1992); an objective of the present NSF grant was to establish the accuracy of the aircraft version, PVM-100A, to measure LWC, as well as PSA.

The following sections describe each of the test activities supported by the NSF grant. Experimental results are presented. The attached APPENDICES contain a reprint of a paper on the present topic presented at the 11th Int. Conf. on Clouds and Precip., Montreal, Aug. 1992 (APPENDIX A); copy of a paper on this topic submitted for publication to Atmospheric Research (Appendix B);

data from the ECN calibration (Appendix C); and data summary of the ASTEX C-131A flights (Appendix D). Conclusions on the performance of the new meter are given in Section 5; and recommendations for future work on instrumentation improvement and data analysis are also listed.

2. CALIBRATION AT ECN

The PVM-100A was taken to the fog-wind tunnel calibration facility at ECN (Netherlands Energy Research Foundation, Petten, The Netherlands), because of earlier similar work (Arends et al., 1992, also see Gerber et al., 1993). This earlier work consisted of comparing the PVM-100 to the LWC filter-method used at ECN to measure LWC. The prior calibration of the PVM-100 against an infrared transmissometer, and the comparison at ECN agreed to within 5%. This excellent agreement between these two fundamental calibration techniques suggested that LWC was being measured accurately with the filter method at ECN. The key difference of the ECN facility as compared to all others, is that the air in the tunnel is preconditioned and servoed to infog conditions to have a relative humidity (RH) close to 100%. This prevents evaporation or growth of droplet samples collected in the filters, and produces ultra-stable and reproducable fogs. The ECN tunnel is relatively low speed, ~ 5 m/s; it cannot simulate aircraft speeds. Given that the output of the PVM instruments are independent of air speed permits this low-speed tunnel to be used to full advantage.

The calibration tests are detailed in Gerber et al. (1993) (Appendix B). The tests are summarized as follows: The PVM-100A, two ECN filter systems, and a FSSP-100 were co-located in the test section of the ECN tunnel. Droplet sprays with various droplet spectra were generated in the ECN facility, and measured by the preceding instruments. The spectra were chosen to cover the range of cloud droplets sizes expected in the atmosphere. This range was sufficiently large to test the large-droplet size limit of the PVM-100A and the FSSP-100. Table 1 summarizes the 10 calibration tests run in the tunnel. Appendix C gives the raw data for the 10 tests.

The analysis of the ECN calibration data is given in Appendix B. The goals of the ECN calibration were to establish scaling constants for the PVM-100A, that are needed to convert instrument output in volts to LWC and PSA, and to confirm the predicted droplet size range over which PVM-100A output was calculated to be linear with typical LWC and PSA values. The major results of this analysis were as follows:

1) The scaling constant and linearity of the LWC channel of the PVM-100A were established with an acceptable accuracy, similar to the accuracy of the previous calibration of the PVM-100 (Arends et al., 1992). This was readily accomplished, because it only required comparing the PVM-100 LWC output to the LWC measured by the ECN filter method that has an established

accuracy record.

Table 1 - Summary of ECN calibration tests of the PVM-100A. See Gerber et al. (1993) for details.

Test No.	Neb. Type	Filter LWC	FSSP LWC	FSSP PSA	FSSP VMD	FSSP Conc.	FSSP Corr.	PVM LWC	PVM PSA
		g/m^3	g/m^3	cm^2/m^3	um	$no./cm^3$		V	V
1	1H	.1376	.132	800	10.2	452	1.135	.0452	.0985
2	2H	.2038	.224	1210	11.7	496	1.149	.0829	.1710
3	3H	.2899	.282	1390	12.9	456	1.137	.1214	.2285
4	1L	.3022	.407	1520	18.9	427	1.127	.1184	.1600
5	2L	.4952	.692	2330	20.5	490	1.147	.2052	.2685
6	2L(p)	.2743	.491	1260	29.4	249	1.072	.0819	.0835
7	1L(p)	.1438	.281	701	30.1	139	1.040	.0434	.0445
8	3L	.7575	.940	2930	21.5	471	1.141	.2880	.3935
9	1W	.4809	.924	1690	40.6	169	1.049	.0939	.0860
10	1W,3L	.9587	1.510	3720	27.8	468	1.140	.3374	.4260

2) The scaling constant and linearity of the particle-surface-area (PSA) channel was also established, but with some unavoidable uncertainty. This uncertainty is a result of attempting to calibrate the PSA channel by comparing it to the output of the FSSP-100 in the ECN tunnel. No other means for measuring droplet surface area were available. The FSSP-100 showed large errors by overestimating LWC in comparison to the filter LWC. The PSA measured by the FSSP was adjusted by a fraction of the LWC overestimate, and used to scale the PSA channel of the PVM-100A. This procedure yielded a scaling constant with small variance. This fact, and some results of the aircraft test (to be discussed in Section 4) suggest that this PSA calibration is reasonably accurate. A calibration of the PSA channel that does not depend on the FSSP-100 is recommended, and is suggested in Section 5.

3. ICING TEST AT NRC

The National Research Council (NRC) of Canada operates a high speed wind tunnel that is used by the atmospheric science community to test instruments designed for aircraft use. This facility, located in Ottawa, has the capability of generating aircraft air speeds to 145 m/s, producing droplet sprays with droplet spectras and LWC typical of the atmosphere, and temperatures between +30 C and -30 C. Support equipment consists

of temperature, pressure, air-speed and water-flow sensors; and a CSIRO hot-wire LWC probe, and FSSP-100 for characterizing the droplets.

The purpose of testing the PVM-100A in the NRC chamber was twofold: It was desirable to expose the PVM-100A probe to aircraft speeds before using the instrument on aircraft, for safety reasons; and it was necessary to test the icing characteristics of the probe. The probe has built into the leading edge of its annulus a 180 Watt anti-icing heater to prevent ice built up due to the impaction of supercooled droplets that could constrict the annulus and give erroneous LWC values. The static temperature limit sought, where ice does not form on the leading edge of the annulus, was -15 C, at an air speed of 80 m/s, and LWC = 0.3 g/m^3.

The tests run in the NRC chamber are summarized in Table 2, and are described as follows:

Table 2 - Tests of the PVM-100A in the NRC high-speed icing tunnel.

Run	Date/Data File	Air Speed m/s	LWC g/m^3	VMD um	Temp. ^oC
1	4 May	80 to 145	Dry		Room
2	5 May/001	80	Dry		20 to -20
3	5 May/003	80	~.5	20	20
	/004	105	~.5	20	20
	/006	130	~.5	20	20
	/008	121	~1.0	20	20
4	5 May/011	120	.97	25	20
5	5 May/013	80	.30	15	20 to -10

Run #1: The air speed was increased from 80 m/s to the limit of the tunnel, 145 m/s, under dry and ambient temperature conditions. At about 140 m/s vibrational noise, traced to the probe, mounted in one wall of the 1 m^2 cross-section tunnel, was detected. It was not possible to determine is this was a natural resonance of the probe, or of the probe-wall combination. At higher air speeds the NRC tunnel generates enormous acoustic energy that couples into the tunnel structure and objects nearby; ear protection is essential.

Run #2: The temperature of the dry tunnel was cycled between about +20 C and -20 C at 80 m/s to determine if thermal stresses affected the probe. Two types of test were run. A slow (1 hr)

change in temperature over this range showed the internal calibration disk in the probe to change ~9% with a long hysteresis. Rapid changes in temperature produced no change. The slow change was traced to small variations with temperature in the position of the internal disk. This disk was irradiated with a minute laser-diode spot; small inhomogeneities in the disk caused the spot to scatter light differently as the disk was thermally forced. Irradiating the disk with a larger laser-diode spot reduced to a large degree this effect.

Run #3, #4: The probe was exposed to various wind speeds (80 m/s - 130 m/s) and LWC (0.5 g/m^3 - 1.0 g/m^3) at ~ 20 C to determine if the optics remained clean, and to see if water leaked into any parts of the probe. No changes in optics, and no leaks were detected.

Run #5: The tunnel temperature was gradually decreased to establish the icing temperature limit of the anti-icing heater on the leading edge of the annulus of the probe. Conditions were LWC = 0.3 g/m^3 and air speed = 80 m/s. A static temperature of -7 C was found as the coldest temperature at which the heater would keep the leading edge of the annulus ice free. This limit was warmer than the -15C that had been desired. This problem was caused by faulty heater design, where the heat, rather than being concentrated near the leading edge, conducted to the rest of the annulus. Redesign of the heater with sufficient insulation between the leading edge of the annulus and the rest of the annulus is expected to give the desired icing temperature limit.

The goals of the NRC tests were met. However it was not possible to compare accurately the PVM-100A to the NRC CSIRO and FSSP-100 probes. The latter was inoperative, while the former gave results that were sometimes erratic and not properly compensated for the tunnel temperature. The CSIRO probe further appeared to show a significant roll off in LWC measured, at wind speeds above 100 m/s. Two plots furnished by NRC showing LWC measured by PVM-100A and CSIRO probes in the tunnel are given in Figs. 2 and 3. The agreement in Fig. 2 may be fortuitous given the disagreement in most of the other comparisons at NRC of these probes. Figure 3 shows the CSIRO (King) probe loses LWC output when the temperature decreases below about -1 C.

4. AIRCRAFT MEASUREMENTS DURING ASTEX

The aircraft test of the PVM-100A was undertaken to determine its ability to operate in an aircraft environment that often includes significant vibration, electrical and RF noise, and large variations in environmental conditions. The PVM-100A was placed on the C-131A aircraft of the University of Washington during the ASTEX. The aircraft flew 16 missions, totaling about 120 hrs., in non-supercooled marine boundary layer clouds in the vicinity of the Azores islands. A wide range of environmental conditions were experienced during the flights, including heavy rain and LWC values in excess of 3 g/m^3.

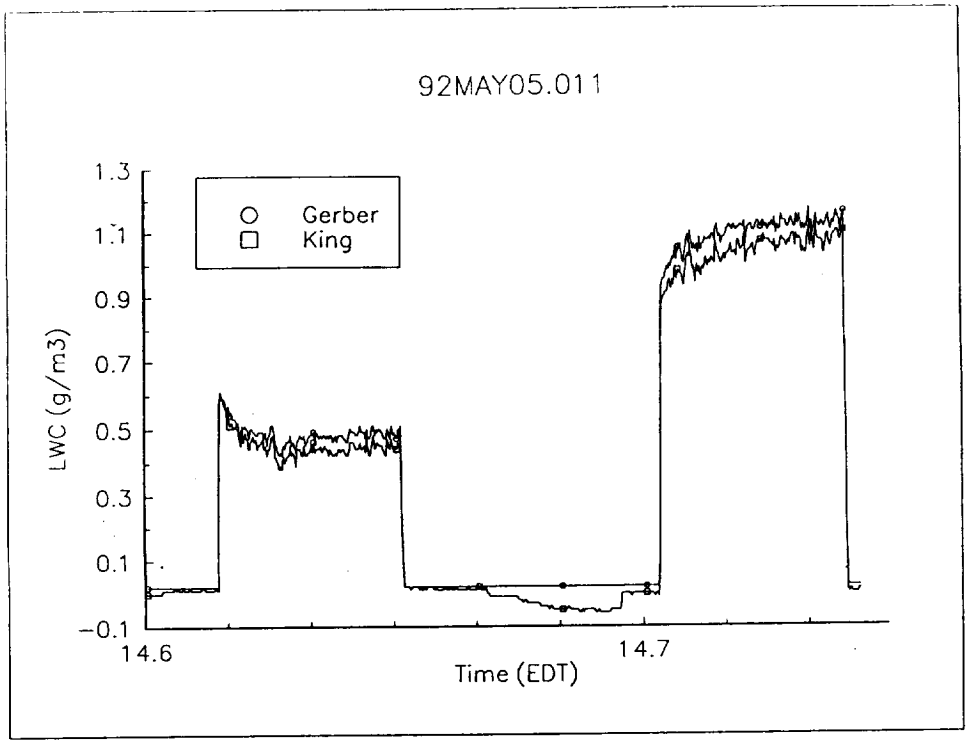

Fig. 2 - Comparison of the CSIRO (King) probe and the PVM-100A in the NRC icing tunnel; part of run #4.

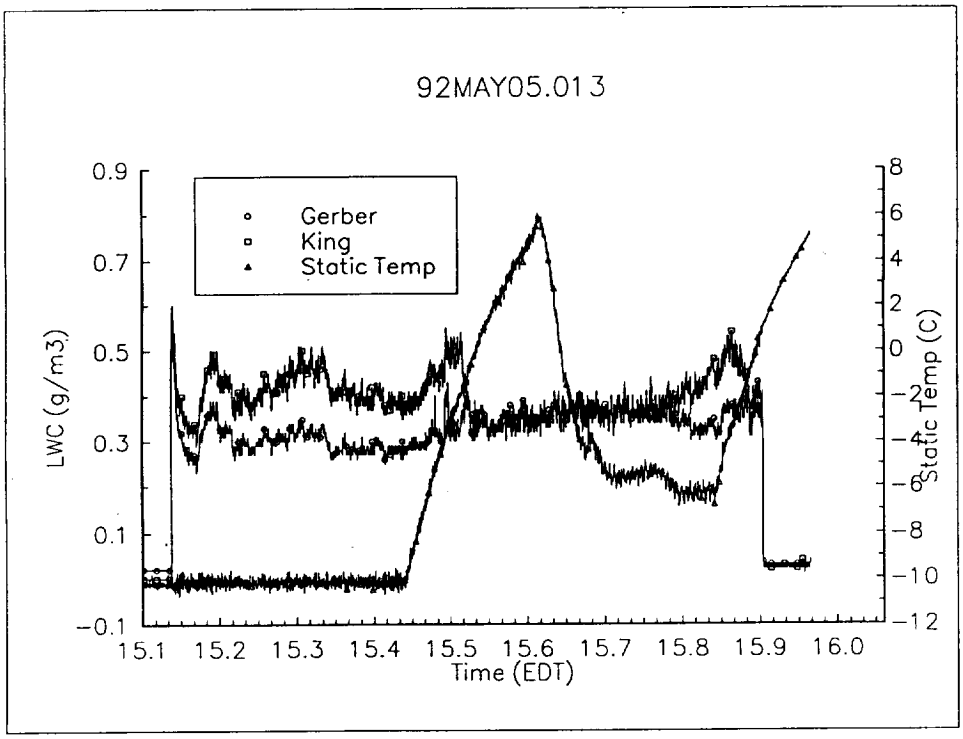

Fig. 3 - Comparison of CSIRO (King) probe and the PVM-100A as a function of temperature; part of test #5.

The PVM-100A was mounted about 3-m behind the nose of the aircraft, and on the lower half of the fuselage. Other University of Washington microphysics sensors were mounted on the fuselage in the same general area about 3-m behind the aircraft nose: a CSIRO (King) hot-wire probe was located 30 cm from the PVM-100, a FSSP-100 was mounted on the bottom of the fuselage, and a JW was located on the bottom half, but other side, of the fuselage. These nearly co-located probes provided an excellent opportunity to intercompare some cloud microphysics probes most commonly used today on research aircraft.

The PVM-100A produced useable data on all C-131A flights. Appendix D lists all the time intervals during the flights when the C-131A was penetrating clouds. This reduced data base consists of ASCII files of 10-Hz and 1-Hz LWC, PSA, and r_e data collected with the PVM-100A during those intervals. The procedure used for data reduction is described, and examples are given of the data files. This data base was submitted to the FIRE/ASTEX data archive. The data reduction was supported in part by NASA funding.

The performance of the PVM-100A during the ASTEX flights was generally very good. Details of the performance follow:

1) During the 16 flights no changes were made to the zero and span adjust controls on the panel of the electronic box of the PVM-100A located inside the aircraft, in order to determine the stability of the instruments electronics and optics. The zero control can be used to subtract offset due to optics that are becoming dirty, and the span control can be used to compensate for changes in the scaling constant required to compensate for changes in instrument sensitivity. This sensitivity can be gauged by momentarily activating the internal calibration disk during the flights. The offset remained unchanged after the 16 flights, indicating that no deterioration of the optics had taken place. The output of the internal calibration disk also remained relatively constant in all 16 flights, indicating that the instrument's sensitivity had remained nearly unchanged. Figure 4 shows the output of the internal calibration for the LWC and PSA channels for times when the calibration disk was activated while the aircraft was incloud. Changes in the calibration voltages amount to less than about 5%.

2) The PSA channel failed to produce an output for interval #27 (see Appendix D). Water had partially filled the end of the probe containing LWC and PSA preamplifiers; the PSA channel was immersed in water. This problem was traced to a missing O-ring seal in that end of the probe.

3) The offset in both LWC and PSA channels varied simultaneously by as much as 5 mv to 10 mv, and it was strongly correlated to other equipment being turned on and off in the aircraft. This indicates that a ground loop was probably affecting the offsets. Future PVM-100A should not reference the output signals to chassis ground, if superior accuracy is

desired. Reference should go to the "ground" of the DC supply, and the outputs recorded in differential fashion.

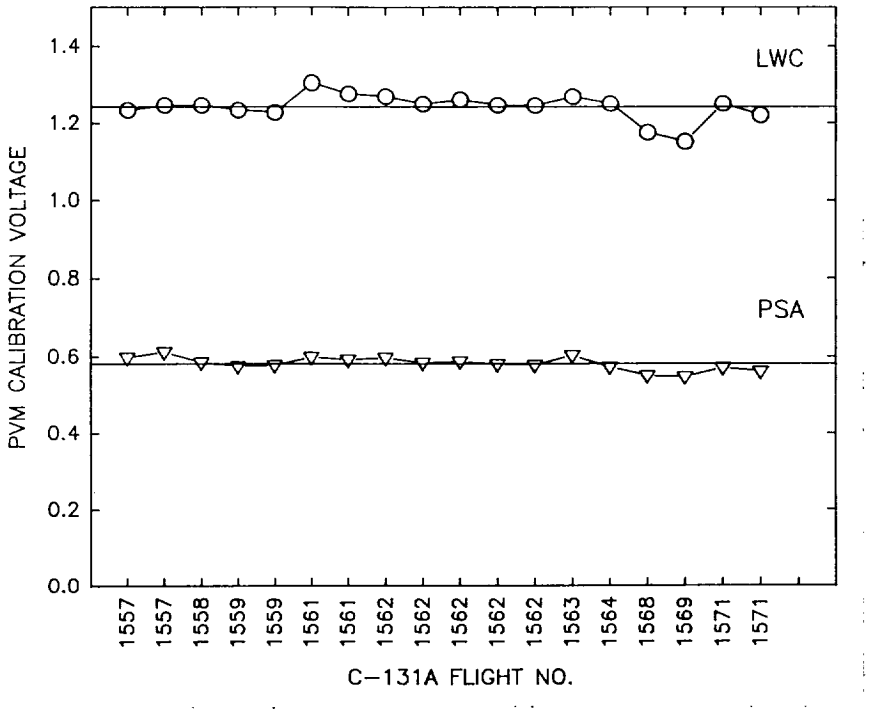

Fig. 4 - Calibration voltages of the PVM-100A during incloud flight of the C-131A aircraft during ASTEX.

4) A small drift in the offsets, with a long e-folding time, was found when the instrument was turned on. This is likely due to the fact that the thermostated heater on the collimating lens of the laser beam is thermally insulated too efficiently from the rest of the optical train in the transmitter section of the probe. A reduction of this insulation should reduce warmup time to less than 5 min.

The data base generated by the PVM-100A during ASTEX has a significant potential for improving the understanding of the physics of marine boundary layer clouds, and clarifying the performance of the microphysics sensors on the aircraft. The scope of the present NSF grant included a preliminary look at the ASTEX data collected with the PVM-100A. The following includes suggestions for analyzing this data base, and gives insights on the significance of this data to addressing current problems in cloud physics:

1) The JW, CSIRO (King) probe, and FSSP-100 all produced nearly continuous data during ASTEX. Detailed intercomparison between these probes and the PVM-100A should produce new

information on the probes' accuracy. See Appendix B for some examples of preliminary intercomparisons. It was found that r_e measured by FSSP-100 and PVM-100A differed by a large amount. This difference is larger than can be accepted in assessing the anthropogenic effect and must be explained; see Appendix B. It may be possible to retrieve accurate FSSP-100 droplet spectra by combining the co-located FSSP-100 and PVM-100A measurements.

2) The radiative effects on stratocumulus cloud-top processes and dynamics must be understood better (Siems et al., 1990). Experimental evidence is needed to substantiate theoretical predictions. It appears that data of the PVM-100A can be used in conjunction with data from other aircraft probes to improve this understanding. There exist cases within the ASTEX data base where the radiation environment above cloud changed markedly (e.g., the existence of a cloud layer above the boundary layer stratocumuli). It is recommended that these cases be investigated, because the effect of radiation can perhaps be quantified.

3) The PVM-100A data is a sensitive indicator of physical properties in regions of the cloud that reflect cloud-top entrainment. For example, Figs. 5 and 6 show r_e and LWC

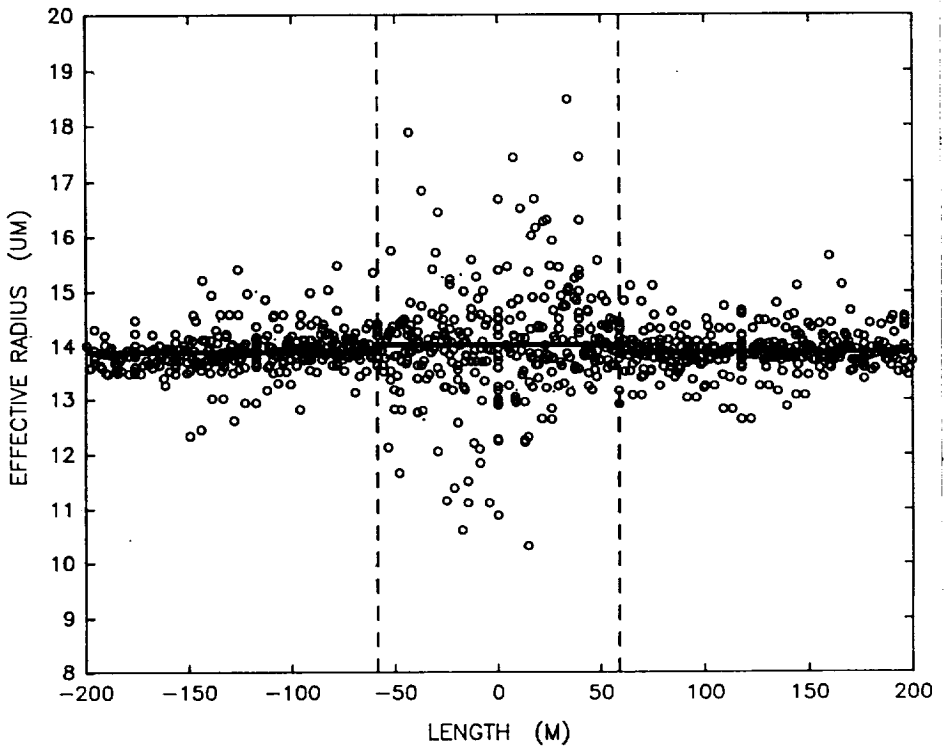

Fig. 5 - Effective droplet radius, r_e, inside and outside entrainment features, normalized to the mean r_e inside and outside, and normalized to the mean feature width given by the dashed lines. Raw data from 25 features.

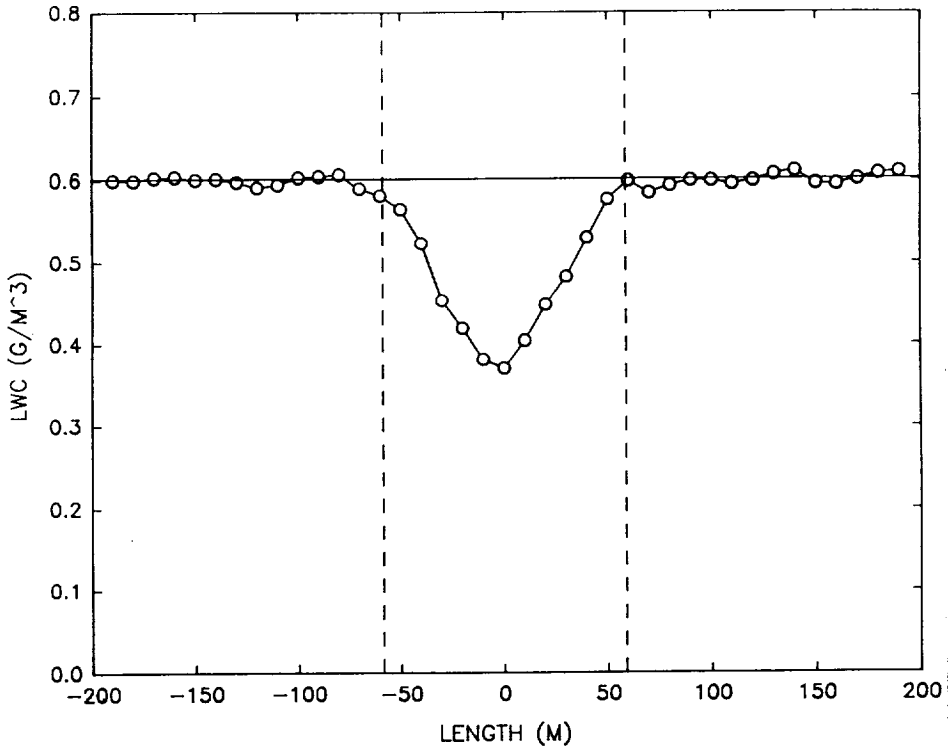

Fig. 6 - Mean LWC inside and outside of the 25 entraiment features in Fig. 5, normalized to the mean feature width given by the dashed lines.

conditionally sampled from the PVM-100A data base that includes the entrained features. The raw data in Fig. 5 represents 25 features sampled near cloud top, normalized to mean feature width and mean r_e. Figure 6 shows the corresponding mean and normalized values of LWC in these features. These data represent a small fraction of the data that can be analyzed in this fashion. The nearly constant mean value (within 1%) of r_e in Fig. 5 agrees with the results of Nichols (1989) who also found the r_e was unchanged in the entrained features, because of the effect inhomogeneous mixing. However, another sample of data in PVM-100A data set does not show the same results as in Figs. 5 and 6. Instead, there is evidence of enhanced droplet growth in "entrained entities" as described earlier by Telford and Wagner (1981) and others. The clarification of entrainment differences is needed.

4) The r_e data base generated by the PVM-100A has attracted a significant amount of attention, because of its usefulness for ground-truthing remote means of retrieving r_e, used by other participants of ASTEX. While this data is now available through the FIRE/ASTEX data base, an effort should be made to organize this r_e data as a function of other parameters measured from the

C-131A. For example, vertical profiles and horizontal traverses of the C-131A should be separated, and the effects of anthropogenic influence on air mass characteristics be established. Statistics of r_e for this data set are also needed.

5. CONCLUSIONS AND RECOMMENDATIONS

The objectives of the present NSF grant, as specified in the proposal, have been met. The PVM-100A was ground and aircraft tested to determine its suitability for use as a LWC, PSA, and r_e sensor on aircraft. To a large degree, the PVM-100 passed the tests successfully. Some aspects of the probe need improvement, they include:

1) The anti-icing heater on the probe should be improved to increase the static-temperature icing limit from -7 C to -15 C.

2) A ground loop affecting the output voltages suggests that the outputs should be measured differentially and not referenced to chassis ground.

3) A small, slow drift in the offsets of the voltage output should be improved by changing the thermal response time of a heater in the transmitter arm of the probe.

The following recommendations are made for further development of the PVM-100A, and for using the data collected by the probe during ASTEX:

1) The PSA channel calibrated in the ECN fog/wind tunnel in Petten, The Netherlands, depended in part on a comparison with the droplet surface area measured with a FSSP-100. Potential errors enter this calibration, because of the uncertainty in the performance of the FSSP-100. Another PSA calibration that does not use the FSSP-100 should be conducted. It is recommended that a vertical sedimentation tunnel using monodisperse glass beads be used for this independent check of the PSA calibration.

2) The 3d channel of the PVM-100A, designed for detecting the ice phase by measuring depolarized light, requires additional research. Measurements to date (funded by Gerber Scientific Inc.) using this channel in a cold chamber with AgI-generated ice crystal clouds showed results that cannot be applied for practical measurement. A lack of sufficient backscatter signal, or ice-crystal habits that do not depolarize to a large degree may be the reason for these negative results. Other arrangements to measure this signal in better specified ice-crystal clouds should be tried. In the present PVM-100A the 3d channel is used to give real-time outputs of r_e, which results by dividing and scaling LWC by PSA. This feature is useful, because of the time delay in sampling the LWC and PSA channels caused by A to D digital data recording.

3. The PVM-100A has the capability of supporting pulse-

height discrimination circuitry simultaneously with the real-time measurements of LWC, PSA, and r_e. This capability would permit the PVM-100A to also measure the spectrum of drizzle droplets and small rain droplets. While other instruments exist to measure drizzle and droplet spectra, the combination of this capability with the existing PVM-100A appears very attractive, because all these paranmeters would them be measured simultaneously by a compact and lightweight probe that accurately measures LWC and r_e.

4. The existing PVM-100A has the potential of providing valuable new data on cirrus ice crystals. It is recommended that the LWC, PSA, and r_e outputs are exposed to ice crystals of known habit, since it may be possible use the PVM-100A to characterize cirrus ice crystals for the radiation community. The present sensitivity of the probe is sufficient to give useful results in cirrus clouds. A calibration of the PVM-100A in the CSU cloud chamber using known ice crystal shapes is highly recommended.

5. The unique data base collected by the PVM-100A during ASTEX has significant potential for improving the understanding of marine boundary layer clouds. Studies using this data should be done for establishing the distribution of r_e as a function of other atmospheric variables measured during ASTEX, for clarifying the effect of radiation on the structure of the clouds, and for determining the causes for the observed large differences in the physical characteristics of entrained entities.

6. REFERENCES

Arends, B.G, Kos., G.P.A., Wobrock, W., Schell, D., Noone, K.J., Fuzzi, S. and Pahl, S., 1992: Comparison of techniques for measurements of fog liquid water content. Tellus, 44B, 604-611.

Baumgardner, D. and Spowart, M., 1990: Evaluation of forward scattering spectrometer probe. Part II: Time response and laser inhomogeneity. J. Atmos. Oceanic Technol., 7, 666-672.

Cooper, W.A, 1988: Effects of coincidence on measurements with a forward scattering spectrometer probe. J. Atmos. Oceanic Technol., 5, 823-832.

Gerber, H., 1991: Direct measurement of suspended particulate volume concnetration and far-infrared extinction coefficient with a laser-diffraction instrument. Appl. Opt., 30, 4824-4831.

Gerber, H., 1992: New microphysics sensor for aircraft use. Proc. 11th Intern. Conf. on Clouds and Precipitation, Montreal, 1992, 942-944.

Gerber, H., Arends, B.G. and Rangno, A., 1993: New microphysics

sensor for aircraft use. Submitted to Atmospheric Research.

King W.D., Parkin, D.A. and Handsworth, R.J., 1978: Hot-wire water device having fully calculable response characteristics. J. Appl. Meteor., 17, 1809-1813.

Nicholls, S., 1989: The structure of radiatively driven convection in stratocumulus. Q. J. R. Meteorol. Soc., 115, 487-511.

Siems, S.T., Bretherton, C.S., Baker, M.B., Shy, S. and Breidenthal, R.E., 1990: Buoyancy reversal and cloud-top entrainment instability. Q. J. R. Meteorol. Soc., 116, 705-739.

Strapp, J.W. and Schemenauer, 1982: Calibration of Johnson-Williams liquid water content meters in a high speed icing tunnel. J. Appl. Meteor. 21, 98-108.

Telford, J.W. and Wagner, P.B., 1981: Observations of condensation growth determined by entity mixing. Pure and Appl. Geophys., 119, 934-965.

7. ACKNOWLEGMENTS

The exceptional effort by Beate Arends and Gerard Kos of ECN during the calibrations at their facility in Petten is gratefully acknowledged. Thanks are due Jack Russel for helping in the installation of the probe on the U. of Washington aircraft, and to Andrew Ackerman of the University of Washington for running the instrument during the C-131A flights. The Department of Meteorology of the University of Washington is also thanked for sharing all the ASTEX data collected with their aircraft. The support of the NASA manager of ASTEX, David McDougal, and of Doris Stroup and Fanny Valladaras during our stay at Santa Maria is much appreciated. The NSF sponsor of this work, Ronald Taylor, is thanked for his support. NASA is also thanked for their partial support of the data reduction.

APPENDIX A

WMO WORKSHOP ON CLOUD MICROPHYSICS AND PRECIPITATION

TORONTO, AUG. 10-14, 1992

11th INTERN. CONF. ON CLOUDS AND PRECIPITATIC

MONTREAL, AUG. 17-21, 19

NEW MICROPHYSICS SENSOR FOR AIRCRAFT USE

H. Gerber

Gerber Scientific Inc., 1643 Bentana Way, Reston, VA 22090 USA

1. INTRODUCTION

The following describes a new optical aircraft sensor, Model PVM-100A, for cloud microphysical measurements. This sensor is based on a redesign of the PVM-100 (Gerber, 1991), an optical sensor used for ground-based measurements of integrated particle volume concentration (termed LWC for clouds). The aircraft sensor differs in its aerodynamic shape, and in the addition of two other channels. One of the channels gives the integrated particle surface area concentration (SAC), which combined with LWC gives the "effective droplet diameter" important in radiation/climate modeling (Slingo, 1989). The second channel determines the presence of the ice phase from depolarization effects.

The PVM-100A has a relatively large sensitive volume (1.25 cm^3), and makes in-situ and real-time measurements independent of air speed. These features permit use of the sensor on high-speed research aircraft, provide spatial resolution of microphysics over distances as small as cm, and give results for small hydrometeor concentrations, including ice crystals.

2. PRINCIPLE OF OPERATION

The measurement of LWC and SAC with the PVM-100A is based on earlier findings that light diffracted out of a light beam into the forward direction by larger particles can be weighted as a function of scattering angle to obtain proportionalities with different moments of the particles' size spectrum, such SAC and LWC [e.g., see Hodkinson, 1966; Wertheimer and Wilcock, 1976; Blyth et al., 1984; Gerber, 1984]. More than half a dozen instruments based on this concept have been built by various groups.

The depolarization of the backscattered light of the linearly polarized laser beam in the PVM-100A is a sensitive indicator of the presence of the ice phase, given that water droplets do not cause depolarization unless multiple scattering is important (Sassen and Liou, 1979; Sassen, 1991).

It may also be possible to use the measure of the depolarized backscatter to estimate the total area and volume fractions in a mixed phase cloud. This is done by relating the relatively constant value of the linear depolarization ratio of ice clouds to measurements of SAC and LWC.

3. INSTRUMENTATION

The PVM-100A consists of a probe (Fig. 1) exposed to the airflow outside the aircraft, and an electronic box placed inside. The optical axis of the probe is parallel to its long dimension, and its

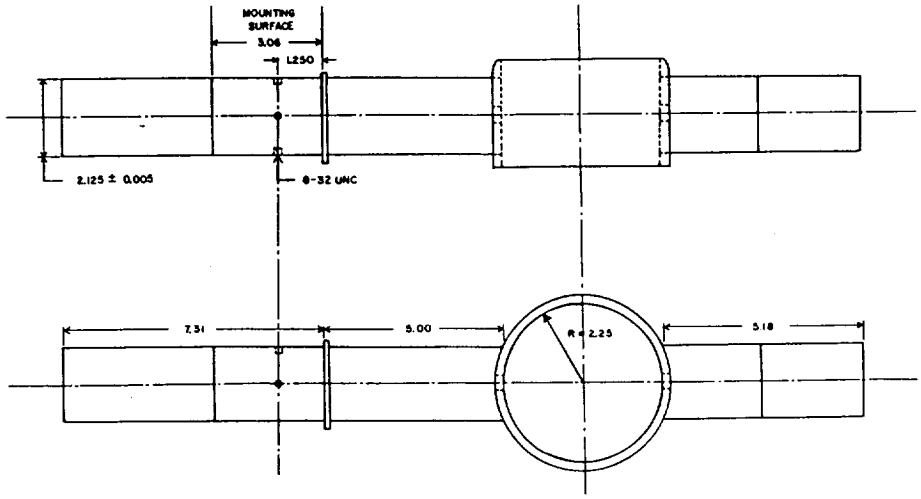

Fig. 1 - Probe of PVM-100A. Top view (upper), front view (lower). Dimensions in inches.

annulus, which contains the scattering volume, faces into the wind direction during use. The probe weighs 3.6 lbs.

The optics of the probe consist of a laser diode light source, collimating optics, and beamsplitter for dividing the scattered light into two components which are weighted to yield SAC and LWC outputs. The weighting is done with spatial filters as described previously (Gerber, 1991). A third detector located in the probes's annulus, and in the plane of polarization of the laser, measures the depolarized backscatter over an angular range of 140 to 170 deg.

The electronics consist of three syncronous detection circuits that output analog voltages proportional to the desired quantities. The reponse of the electronics permit a measurement rate of 0 to 5000 Hz. Calibration consists of an internal light diffusing disk that can be activated with Logic 1.

The leading edge of the probe's annulus contains 140 Watt heaters for icing protection. Additional heaters are used to protect the optics from condensation.

LWC is measured over a range of 0.001 - 10 g/m^3; SAC is measured over 5 - 5000 cm^2/m^3; and the range for the depolarization measurement is yet to be determined.

4. CALIBRATION AT ECN

The PVM-100A was calibrated in the low-speed cloud/wind tunnel at ECN (Netherlands Energy Research Foundation) by comparing its output to gravimetric filter measurements of LWC for various cloud densities and droplet spectra. Co-located FSSP-100 measurements were also made. A schematic of the ECN facility is shown in Fig. 2. Its ability to measure LWC in warm clouds with the filter method over a wide range with an accuracy of better than 10% depends on precisely setting RH to 100% in the cloud to avoid growth or evaporation of droplets in the filters. This is achieved by thermally servoing humidifier temperature to cloud temperature; and by collecting droplets isokinetically in prewetted hydrophobic filters.

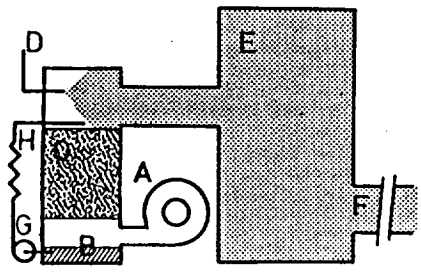

Fig. 2 - Schematic of cloud/wind tunnel at ECN. A (blower), B(water resevoir), C(humidifier), D(fog generator), E(mixing chamber), F(tunnel, 5m), G(water pump), H(heater) [from Mallant (1988)]

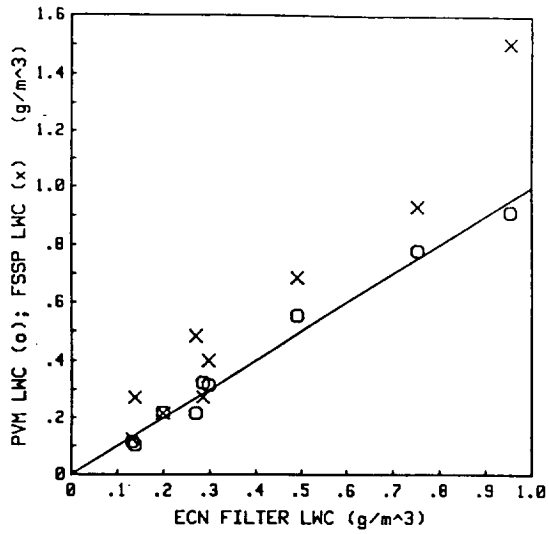

Fig. 3 - Comparison of LWC measurements in ECN cloud chamber with filter method, PVM-100A (o), and FSSP-100 (x).

Figure 3 compares ECN filter, FSSP-100, and PVM-100A LWC measurements for atomizer droplet spectra with mmd ranging from 10.2 um to 30.1 um. The approximately linear relationship between PVM-100A and filter measurements shows that the PVM-100A has the required independence of droplet size over this range of mmd, and the linear relationship can be used to determine the scaling factor for field measurements of LWC with the PVM-100A. LWC values determined by integrating the droplet spectra measured with the FSSP-100 show less of a linear relationship with the filter results, and are as much as 90% larger. For large droplets generated with a paint sprayer (with an unknown number of drops larger than the 95-um limit of largest bin in FSSP-100, and an unknown mmd greater than 40 um), the PVM-100A underestimates LWC, and the FSSP-100 overestimates LWC as compared to the filter measurements.

The SAC channel in the PVM-100A was calibrated using the FSSP-100 integrated droplet surface area data corrected by referencing the FSSP-100 LWC data to the filter LWC:

$$\underset{\text{(corrected)}}{\text{FSSP(AREA)}} = \underset{\text{(measured)}}{\text{FSSP(AREA)}} \times \left(\frac{\text{FSSP(LWC)}}{\text{FILTER(LWC)}} \right)^{-2/3}$$

This approach assumes that correcting for the various possible error sources in the FSSP-measured droplet spectra (see Baumgardner and Spowart, 1990), is equivalent to adjusting the droplet number density uniformly across the spectra. For the present experiment this approach works reasonably well as shown in Fig. 4, where PVM-100A and corrected FSSP-100 total surface areas are compared. The standard deviation of the variability about a

linear relationship in Fig. 4 is larger by a factor of about 2 when using uncorrected FSSP-100 data. The linear relationship in Fig. 4 is used to determine the scaling constant for the SAC channel.

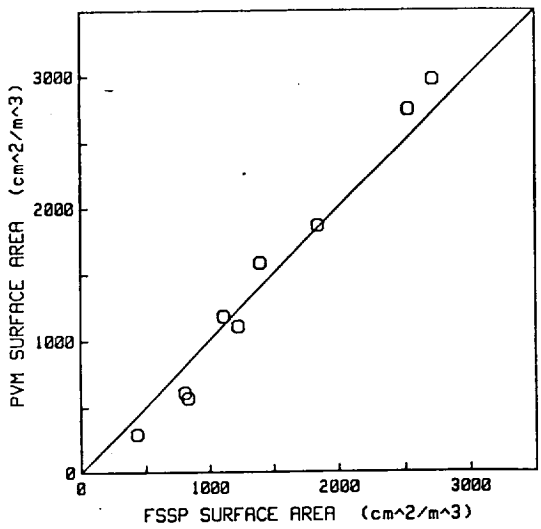

Fig. 4 - Comparison of total droplet area concentration (SAC) measured with PVM-100A and FSSP-100.

5. CONCLUSIONS AND ADDITIONAL EVALUATIONS

The calibration at ECN has shown that the PVM-100A is capable of LWC measurements within an accuracy of about 10% for droplet mmd from 10 um to 30 um in warm clouds. The calibration of the SAC channel is probably less accurate, because it depends in part on the unknown accuracy of the method for correcting the FSSP-100 data.

Additional evaluation of the PVM-100A will consist of placing the instrument in a high-speed icing tunnel where aircraft environmental conditions with repect to temperature extremes and LWC contents can be simulated. Measurements from aircraft are also scheduled.

ACKNOWLEDGEMENTS

Gabor Vali of U. of Wyoming is thanked for his important contribution to the design of the aircraft sensor. Beate Arends and Gerard Cos of ECN for the excellent calibration work, and NSF for partial support of this work under ATM-9207345.

REFERENCES

Baumgardner, D., and M. Spowart, 1990: Evaluation of the forward spectrometer probe. Part III: Time response and laser inhomogeinity limitations. J. Atmos. Oceanic Technol., 7, 666-672.

Blyth, A.M., A.M.I. Chittenden and J. Latham, 1984: An optical device for the measurement of liquid water content in clouds. Q.J.R. Meterol. Soc., 110, 53-63.

Gerber, H., 1984: Liquid water content of fogs and hazes from visible light scattering. J. Climate and Appl. Meteorol., 23, 12-7-1252.

Gerber, H., 1991: Direct measurement of suspended particulate volume concentration and far-infrared extinction coefficient with a laser-diffraction instrument. Appl. Opt., 30, 4824-4831.

Hodkinson, J.R., 1966: "The optical measurement of aerosol" in Aerosol Science, C.N. Davies, Ed., Academic Press, New York.

Mallant, R.K.A.M., 1988: "A fog chamber and wind tunnel facility for calibration of cloud water collectors" in Acid Deposition at High Elevation Sites, M.H. Unsworth and D. Fowler Eds., Kluwer Academic Publishers, The Netherlands.

Sassen, K., 1991: The polarization lidar technique for cloud research: A review and current assessment. Bul. Amer. Meteorol. Soc., 72, 1848-1866.

Sassen, K. and K.-N. Liou, 1979: Scattering of polarized laser light by water droplet, mixed-phase and ice crystal clouds. Part II: Angular depolarization and multiple-scattering behavior. J. Atmos. Sci., 36, 852-861.

Slingo, A., 1989: A GCM parameterization for the shortwave radiative properties of water clouds. J. Atmos. Sci., 46, 1419-1427.

APPENDIX B

Submitted to **ATMOSPHERIC RESEARCH**

New Microphysics Sensor for Aircraft Use

H. Gerber

Gerber Scientific Inc., 1643 Bentana Way, Reston, VA 22090 (U.S.A.)

B.G. Arends

Netherlands Energy Research Foundation (ECN), P.O. Box 1, 1755 ZG Petten (The Netherlands)

A. Ackerman

Department of Atmospheric Sciences, AK-40, University of Washington, Seattle, WA 98195 (U.S.A.)

ABSTRACT

A new optical sensor, PVM-100A, for aircraft cloud-microphysical measurements is described. This sensor is an adaptation of an instrument, PVM-100, used for ground-based measurements of LWC. The new sensor measures the liquid water content (LWC), the integrated particle surface area (PSA), and the effective droplet radius of cloud droplets. The measurements are simultaneous, are made on a cloud volume of 1.25 cm^3, are made in situ and in real time, and have a maximum rate of 5 KHz.

The new sensor was calibrated in the fog-wind tunnel at ECN, Petten, The Netherlands. The LWC and PSA channels of the sensor were compared to gravimetric measurements of droplets collected

in filters, and to a FSSP-100, respectively. The LWC calibration gave accurate results, and showed a linear response of the PVM-100A to LWC for droplet spectra with volume median diameters (VMD) up to about 25 μm. The results of the PSA calibration were less certain, because of uncertainties in the behavior of the FSSP-100.

The PVM-100A was flown on the University of Washington C-131A aircraft during the one-month ASTEX (Atlantic Stratocumulus Transition Experiment) program, where marine boundary-layer clouds were investigated near the Azores. The new sensor operated in a stable fashion during the 16 flights, and is compared to data produced by co-located probes consisting of the Johnson-Williams hot-wire probe, CSIRO (King) hot-wire probe, and FSSP-100. The comparison shows the hot-wire probes unable to resolve features in broken clouds, because of insufficient time response, it shows the FSSP-100 underestimating LWC when either LWC or droplet sizes are large, and it shows a large difference in the effective droplet radius measured by the FSSP-100 and PVM-100A. The latter reflects the time-response error of the uncorrected FSSP-100 that causes large underestimates of droplet sizes at aircraft speed. The PVM-100A data appeared physically consistent throughout the ASTEX flights, and produced a nearly continuous 10-Hz data set of LWC, PSA, and effective droplet radius.

INTRODUCTION

We describe the principle of operation, the configuration, and the testing of a new microphysics sensor, PVM-100A, designed

for aircraft use (Gerber, 1992). This two-channel sensor measures optically and in situ the liquid water content (LWC) and the total particle surface area (PSA) of cloud droplets. It thus also provides the effective droplet radius, r_e, because $r_e \propto$ LWC/PSA. The value of r_e in clouds is useful in parameterizing the radiative effect of clouds (Slingo, 1989); and the reduction of r_e in clouds due to anthropogenic influences may counter in part global warming due to the increase in CO_2 (Slingo, 1990).

The new sensor is an adaptation of a similar instrument, the PVM-100, used for ground-based measurements of LWC; see Gerber (1991) and Arends et al. (1992). Both instruments utilize light diffracted in the forward direction by cloud droplets to measure integrated droplet properties. The PVM-100A differs primarily from the PVM-100 in that its probe is designed for mounting on the outside of aircraft, its faster electronics cope with aircraft speeds, and its two channels simultaneously measure LWC and PSA for the same cloud volume (the newer PVM-100 also include this capability.)

The development of the PVM-100A is an attempt to improve the accuracy of measuring LWC and PSA of cloud droplets from aircraft. Present instruments for measuring LWC include the Johnson-Williams (JW) hot-wire probe, the CSIRO hot-wire probe (also called the King probe; King et al., 1978), and the Forward Scattering Spectrometer Probe (FSSP-100; Particle Measuring Systems, Boulder, CO). The JW has a significant dependence on air

speed (Strapp and Schemenauer, 1982); the King probe (KP) agrees to within 15% of values calculated using the icing-cylinder calibration technique (King et al., 1985) for droplet sizes within its design range (Biter et al., 1987); and the FSSP-100 gives LWC with the best accuracy by applying corrections for coincidence and deadtime losses, and time-response and laser-inhomogeneity errors (e.g., see Baumgardner et al., 1985; Cooper, 1988; Brenguier and Amodei, 1989;, Brenguier, 1989; Baumgardner and Spowart, 1990.) Given that existing FSSP-100 differ from each other means that these corrections cannot be entirely adequate unless the variables of each instrument are identified (Cooper, 1988; Baumgardner and Spowart, 1990). In contrast to the preceding three techniques, the PVM-100A does not depend on the rate at which droplets either impact or pass through the instrument; its output is independent of air speed. The PVM instruments look at many droplets simultaneously in a cloud volume about 50,000 larger than the sensitive volume in FSSP-100, where droplets are measured optically individually and summed for LWC. These differences permit the PVM to measure LWC more accurately; the accuracy of the PVM-100 is better than 10%, see below.

The following decribes the calibration of the PVM-100A in the CHIEF (Chamber for Investigations with Equilibrated Fog; Mallant, 1988) located at Netherlands Energy Research Foundation (ECN), Petten. The PVM-100A is compared to LWC measured with the filter method, as done previously with the PVM-100 (Arends, et al., 1992). The calibration of the PSA channel has inherently greater uncertainty, because it relies on comparing in the chamber the

PVM-100A with a FSSP-100. Also described are results of measurements with the PVM-100A during ASTEX (Atlantic Stratocumulus Transition Experiment), where the instrument was mounted near other cloud microphysical probes on the University of Washington's C-131A during the 4-week experiment in June 1992. Comparisons are shown between the JW, KP, FSSP-100 and PVM-100A.

INSTRUMENTATION

The probe for the PVM-100A is shown in Fig. 1. It consists of a 11.4-cm-diameter annulus which faces into the wind direction during flight. The longer cylindrical tube to the left of the annulus contains the laser-diode light source and collimating optics, and mounting holes for attaching the probe to an aircraft pylon or another mounting arrangement. The shorter tube on the right contains the optics and detectors for the LWC and PSA channels. The laser beam traverses the annulus where it irradiates a volume of 1.25 cm^3. The probe weighs 1.8 Kg. The probe is connected by cable to an electronic box located inside the aircraft. The electronics use synchronous detection to isolate the signals produced by light scattered by the droplets, the signals are scaled, and three analog outputs for LWC, PSA, and r_e are produced. The maximum output frequency is 5 KHz.

The principle of operation of the PVM is illustrated in Fig. 2. Cloud droplets (or other particles such as ice crystals) scatter light into the near-forward direction into a lens that focuses the scattered light onto a variable-transmission filter and sensor for each channel. This arrangement closely resembles a

class of commercial instruments usually called "laser-diffraction particle-sizing instruments"; see Azzopardi (1979) and Hirleman (1984). These instruments differ in that they utilize a segmented multi-element sensor from which outputs are mathematically inverted to derive droplet spectra. The PVM arrangement uses instead the variable-transmission filter which has built into it a transmission function also derived by inversion to directly output LWC or PSA. Similar direct means for measuring such integrated properties of suspended particles have been described in the literature for many years (e.g., Stetter, 1949; Breuer, 1960; Wertheimer and Wilcock, 1976; Blyth et al., 1984; Gerber, 1984.)

The method used to establish LWC and other desired responses of the PVM is fully described in Gerber (1991), and will only be summarized in the following for the case of LWC:

The equation for LWC is given by

$$LWC = \frac{4\pi\rho}{3} \int r^3 \, n(r) \, dr \qquad (1)$$

where r is the droplet radius, $\rho = 1.0$ is the droplet density, and n(r) is the droplet size spectrum.

If the scattered-light flux measured by the LWC sensor (see Fig. 2) for droplets of radius r is given by F(r), then the equation

$$F(r) = k_1 \, r^3 \qquad (2)$$

must be shown to be valid for the PVM to properly measure LWC; k_1

is a constant.

If the filter consists of annular segments identified by the letter i, then

$$F(r) = \sum_{i=1}^{N} f_i(r)\, T_i \qquad (3)$$

where $f_i(r)$ is the flux of diffracted light incident on i, T_i is the transmission of filter annulus i, and N is the total number of annuli.

The expression for

$$f_i(r) = k_2\, l_i\, r^2\, [(J_o^2 + J_1^2)_{i1} - (J_o^2 + J_1^2)_{i2}] \qquad (4)$$

is the same as given by Swithenbank et al. (1976), except for the factor l_i which compensates for vignetting effects in the PVM; k_2 is a constant. J_o and J_1 are Bessel functions of the first kind (zeroeth and first order, respectively), and the indices 1 and 2 of the Bessel functions denote boundaries of each annulus ring.

In order to achieve the required relationship shown in Eq.(2), the proper function of T_i must be found in Eq. (3). This is done by mathematically inverting Eq. (3) to determine T_i. Equation (3) is the discrete form of a Fredholm integral of the first kind which is inverted with the condition that Eq. (2) holds. A resulting curve of T_i vs. annulus number is shown in Gerber (1991). The filter with this distribution of T_i gives a predicted bandpass of about 4-μm to 45-μm droplet diameter over which the reponse of the PVM is linear with LWC. Outside of this range the response gradually rolls off with 50% points at about 2

μm and 70 μm. A filter with this response is presently used in both the PVM-100A and PVM-100. Filters with other linear bandpasses that cover smaller or larger droplet-size ranges can be designed.

CALIBRATIONS AT ECN

1. CHIEF Fog Chamber

The CHIEF fog chamber at ECN. Petten, The Netherlands is illustrated in the schematic in Fig. 3. Ambient air enters A and passes into the ~4-m^3 chamber C where water trickling over many porous ceramic rings is used to humidify the air to near 100% relative humidity (RH). Atomizers add droplets to the flow at D, which enters the 20-m^3 chamber E where the air and droplets mix. The flow then passes through a 5-m long test section F with a 50-cm by 50-cm cross section. Instruments to measure droplet properties are placed about halfway along F. A key feature of the chamber is that the temperature in F is used to regulate the water temperature in the humidifier C with the heater H so that the RH in the chamber remains stable, and so that the fogs generated in the chamber also remain stable for as long as the droplet generators at D produce constant outputs.

The fogs are characterized in F by measuring the LWC with the filter method, and measuring the droplet spectra with a FSSP-100. Two filter systems are run side by side as a check of the measurement procedure. The filters consist of hydrophobic Pall filters placed in housings that face the flow. Air is drawn

through the filters isokinetically at 2.15 m/s.; and the flow rate through the filters is measured with calibrated gas meters. The filters are conditioned in the operating chamber for at least 2 hrs. before LWC is measured by weighing the filter both before and after a specified time interval, generally on the order of 1 hr. The constant high RH in the chamber, and this filter-sampling procedure should minimize LWC measurement errors due to evaporation or growth of droplets collected in the filter. Such errors may be important where the filter method is used under ambient conditions where RH can be subsaturated or supersaturated (e.g., see Valente, et al., 1989).

The FSSP-100 is located near the filters in the test section F. Droplet spectra measured during the present calibration of the PVM-100A are shown in Fig. 4. These spectra are typical of those measured in a previous calibration (Arends et al., 1992), with the exception that spectra were previously limited to droplet volume median diameters (VMD) 20 μm or smaller. In the present calibration larger VMD were used in order to test the limit of large-particle sensitivity of the instruments. The present calibration also differed from the preceding calibrations in that larger LWC values up to about 1 g/m^3 were generated in the CHIEF. Each spectrum in Fig. 4 is a normalized average of three sets of tests in the chamber, where the sets have similar VMD near 10 μm (tests 1, 2, 3), 20 μm (tests 4, 5, 8), and 30 μm (tests 6, 7, 10); see Table 1.

2. Calibration of PVM-100

The previous calibration of the PVM-100 for LWC is briefly reviewed here, because those results have bearing on the method of analyzing the present calibration of the PVM-100A. The PVM-100 was calibrated by comparing it to infrared extinction measurements made through fogs with various droplet spectra in the Calspan Corp., Buffalo environmental chamber (Gerber, 1991). Given that infrared extinction at ~11-μm radiation was predicted to be proportional to LWC according to Mie theory (Chylek, 1978), and verified as such (Pinnick et al., 1979; Gertler and Steele, 1980; Nolan and Jennings, 1987), permitted the scaling constant relating voltage output of the PVM-100 and LWC to be determined.

The PVM-100 was also compared to the filter method as described by Arends (1992). Figure 5 shows this comparison. K, the mean ratio of LWC(Filter)/LWC(PVM-100) for the data in this plot, is equal to 1.05 with sample standard deviation s = 0.0845. This difference indicates that the PVM-100, as calibrated against the infrared transmissometer, gives LWC values smaller by 5% on the average than LWC determined with the ECN filters. The value of K depends in part on the relationship between LWC and infrared extinction; the relationship given by Nolan and Jennings (1987) is used here. The correlation coefficient between data sets in Fig. 5 is .991, and K differ by less than 5% for the two values of VMD. This good agreement of LWC measured independently by two fundamental calibration techniques suggests that LWC is being measured accurately by the PVM-100 over the given VMD range.

3. Calibration of PVM-100A

The procedure for calibrating the new aircraft probe, PVM-100A, consists of first producing a reference voltage output for each channel that can be easily reproduced. This is done by placing a light diffusing disk against the receiver-tube aperture, and adjusting the instrument's gain to choose a reference voltage. The reference voltages chosen for the PVM-100A were .075 V for the LWC channel, and .500 V for the PSA channel. The next step is to compare the output of each channel to a standard method of measuring LWC and PSA to determine scaling constants K_1 and K_2 required to scale the PVM-100A voltages:

$$LWC(\text{Standard; } g/m^3) = PVM(\text{Volts}) \times K_1 \qquad (5)$$

$$PSA(\text{Standard; } cm^2/m^3) = PVM(\text{Volts}) \times K_2 \qquad (6)$$

The ECN filter method is used as the standard for LWC. The values of LWC measured by the filters, Table 1, are averages of the two adjacent filters used simultaneously for each test. The mean difference between filters was 2.86%. K_1 is determined by averaging K_1 values calculated for some of the tests listed in Table 1. Given the previous good agreement between LWC measured by the PVM-100 and the ECN filter method for VMD ~ 20 μm and smaller, this averaging is limited to the tests in Table 1 where VMD is ~10 μm (tests 1, 2, 3) and ~20 μm (tests 4, 5, 8). The value of K_1 determined in this fashion is 2.58 with s = 0.241. Figure 6 shows the relationship between LWC measured by the filter and PVM-100A after this scaling constant is applied to all

the PVM-100A measurements. The PVM-100A LWC with VMD ~10 μm and ~20 μm shows a highly linear relationship with filter LWC as also noted in the previous calibration. Tests 6, 7, and 10 for which VMD ~30 μm show that the PVM-100A underestimates the filter LWC by a mean value of 18%. This value is reasonably close to the expected underestimate of ~15%, predicted by applying the particle-size bandpass of the LWC filter used in the instrument to the measured droplet spectrum (Fig. 4). Test 9 shows an underestimate in the PVM-100A LWC of ~50%. For this test, the Wagner nebulizer produced some droplets that were beyond the 95-μm diameter limit of the FSSP-100. Thus the measured VMD of 40.6 μm for this test is an underestimate of the true unknown value of VMD.

The FSSP-100 is used as the standard for determining the scaling constant K_2 for PSA. This requires that the FSSP-100 produces accurate values of PSA. We see from Fig. 6 that the FSSP-100 significantly overestimates LWC for most of the tests, so that values of PSA calculated from the FSSP-100 droplet spectra will be inaccurate and will also show overestimates. This trend in LWC measured by the FSSP-100 was noted previously by Arends et al. (1992) during the calibration where FSSP-100 and PVM-100 were compared; one of us (B.G.A.) is presently investigating this result. The magnitude of the overestimate in LWC, given by the ratio of the LWC measured by the FSSP-100 and the filter, increases as a function of VMD; see Fig. 7. The tests show a linear increase in this ratio with VMD, except for test 9, which is not included in the subsequent analyses.

The value of K_2 is estimated by comparing the voltage output of the PVM-100A PSA channel to values of PSA measured with the FSSP-100 and corrected for the overestimates. Given that this FSSP-100 was exposed to monodisperse glass beads, which showed proper sizing by the instrument, suggests that the error is related to concentration overestimates.

The determination of the PSA correction consists of an inversion problem as shown by the following integral for LWC, which should be compared with Eq.(1):

$$\text{FILTER(LWC)} = \frac{4\pi}{3} \int c(r,n)\ r'^3\ n'(r)\ dr \qquad (7)$$

where the incorrect volume size spectra measured by the FSSP-100 is given by $r'^3 n'(r)$, $c(r,n)$ is the correction function, and FILTER(LWC) is assumed to be the correct measure of LWC. It is necessary to solve for $c(r,n)$ which can then be used to find the correction for the PSA integrals of the FSSP-100 data.

If we assume that n is correct, and that the overestimate is in r (contrary to the glass-bead evidence), that is $n'(r) = n(r)$, then $c(r,n) = r^3/r'^3$. If we further assume that r and r′ are related by $r = r' \times [\text{FILTER(LWC)/FSSP(LWC)}]^{1/3}$, then $c(r,n)$ is given by the reciprocal, FILTER(LWC)/FSSP(LWC), of FSSP-100 LWC error. This gives $[\text{FILTER(LWC)/FSSP(LWC)}]^{2/3}$ as the correction for the surface integrals. The corrected PSA values are shown in Fig. 8 (solid circles). The mean value of K_2 determined with Eq. (6) from the corrected values of PSA is 7,700 with s = 749.

If we now assume that the FSSP-100 accurately measures r, but instead overestimates n(r), that is $r' = r$, then $c(r,n) =$

$n(r)/n'(r) = g(r)$, where $g(r)$ is an unknown function of r. Given that an integral similar to Eq. (7) exists for each of the 9 tests, which must each include the same $g(r)$, it is possible to estimate the dependence of $g(r)$ on r. Figure 9 shows a second-order polynomial fitted to data consisting of y = FSSP VMD and the ratio x = FILTER(LWC)/FSSP(LWC). The data point y = 100 um, x = 0 is arbitrarily added; and x is assigned a value of 1.0 for y < 11 um. The correction function $g(r)$ is given by the polynomial in Fig. 9 solved for x, that is $x = f(y) = g(r)$, which applies to both the LWC and PSA integrals of the FSSP-100. A test of the fit of $g(r)$ is to apply $g(r)$ to each size bin of the FSSP-100 LWC spectra for all the tests, and to see if the correct filter LWC result. The mean difference between the corrected LWC and the filter LWC is within 1% with a correlation coefficient of .995. When $g(r)$ is applied to the FSSP-100 PSA integrals, corrected PSA values result (Fig. 8, open circles) from which a mean value of $K_2 = 7{,}584$ with s = 1634 is found. The close agreement of K_2 found for the preceding two methods suggests that the PSA correction is independent on whether r or n causes the overestimates.

For the preceding estimates of K_2 we have applied to the FSSP-100 data in Table 1 coincidence and dead-time concentration corrections (listed in Table 1) according to the formulation given by Baumgardner et al. (1985). The influence of these corrections on the value of K_2 is small; however, the effectiveness of the corrections are evident in that they significantly reduce the corresponding value of s. Given the relatively slow air speed of 27.4 m/s through the FSSP-100 during the tests, the correction for time-response error given by

Baumgardner and Spowart (1990) was not applied.

An independent validation of the preceding PSA calibration is recommended. Exposing the PVM-100A to monodisperse glass beads in a vertical sedimentation tunnel is suggested as a good approach for such a calibration, because the output of the instrument is independent of the speed of the particles.

AIRCRAFT MEASUREMENTS

The PVM-100A was flown on the University of Washington's C-131A during the ASTEX Project in June 1992. It was mounted on the lower half of the fuselage about 3-m behind the nose of the aircraft, and in close proximity to a JW hot-wire probe, a King hot-wire probe, and another FSSP-100. The C-131A flew 16 missions during ASTEX, with a total of about 120 hrs. flight time. Conditions experienced during the flights included heavy drizzle and rainfall, droplet concentrations from about 50/cm^3 to 2000/cm^3, and clouds with LWC of more than 3 g/m^3. The PVM-100A operated in a stable fashion during the flights, with minimal changes in optics and electronics. The following is not intended to provide an in-depth comparison of the preceding probes, but will be limited to presenting a few examples of the collected data.

Figure 10 compares LWC measured by the JW, King probe, FSSP-100, and PVM-100A during a short segment of a flight passing through broken stratocumuli. The sampling rate of the data recording system aboard the C-131A was 10 Hz. The JW produced the smallest values of LWC. Both commercial hot-wire probes showed hysteresis in their response time, so that inter-cloud gaps were not resolved in comparison to the output of the faster-responding

PVM-100A.

Figure 11 compares LWC measured by the King probe, FSSP-100, and PVM-100A during an ascent through a stratocumulus layer that was noteworthy for showing a small amount of entrainment at its upper surface. This layer differed from nearly all others in that local regions of lowered LWC, which are indicative of the entrainment into cloud top of drier air, where minimal. Also, the droplet concentration in this layer was unusually stable. The lack of significant entrainment in this layer may have been due to the known existence of a higher cloud layer shielding this layer from radiative effects that influence entrainment. This layer should show a LWC profile that is nearly adiabatic, because of the low entrainment. The King probe significantly underestimates the adiabatic LWC profile; this probe generally gave better results, but was erratic on occasion. The FSSP-100 data, to which no corrections were applied, shows a typical rolloff in LWC seen when either LWC increases to larger values or the droplet spectrum shifts to larger droplet sizes. These trends are symptomatic of the aircraft use of the FSSP-100, and are opposite to the trend found for the low-speed use of the ECN FSSP-100 described in the preceding calibration. The PVM-100A shows the best agreement with the adiabatic LWC profile in Fig. 11. This is indirect evidence that the LWC calibration was done correctly, under the assumptions that cloud-top entrainment was in fact minimal, and that the cloud layer was horizontally homogeneous over the distance required for the aircraft to complete the profile.

Figure 12 compares r_e (K_1 = 2.58, K_2 = 7,700) measured by the PVM-100 and the University of Washington FSSP-100 (uncorrected) in marine boundary layer clouds during ASTEX. The data represent 1-min. averages of r_e taken from 500 Km of incloud flight distance (average aircraft speed was 83 m/s), and represent a wide range in droplet spectra and concentrations; cases with drizzle are not included. The difference in Fig. 12 between r_e measured by FSSP-100 and PVM-100A is highly correlated, and shows a regression relationship where the measurements differ by approximately a constant factor. This result is consistent in magnitude and direction with the "time response and laser inhomogeneity" errors of the FSSP-100 used at aircraft speed as calculated by Baumgardner and Spowart (1990); see horizontal bars in Fig. 12, also see their Fig. 5. They found that the FSSP-100 underestimated droplet size by approximately a constant factor of the actual size at a simulated airspeed of 80 m/s. This means that this factor, although probably different for various FSSP-100, because of inherent instrumentation differences, will appear approximately unchanged in the calculation of r_e, and will be largely independent of droplet concentration.

This result suggests that flying both the FSSP-100 and PVM-100 together on the same research aircraft may significantly improve the accuracy of the droplet specta measured by FSSP-100 by correcting them with PVM-100A measurements. The suggested procedure would partition time-response and concentration error corrections with the following sequence:

1) The factor difference in r_e, established by comparing PVM-100A and FSSP-100 r_e measurements, is used to correct the FSSP-100 droplet size spectrum.

2) The LWC measured by the PVM-100 is used to scale the FSSP-100 LWC, thus correcting the FSSP-100 concentration errors.

3) A correction is applied to the droplet spectrum to eliminate the small number of "large droplets" caused by the coincidence of smaller droplets in the FSSP-100 sample volume (Cooper, 1988).

The accuracy of this procedure depends on the accuracy of the PVM-100A calibration and the results of Baumgardner and Spowart (1990). At the least, the high expected precision of the PVM-100A, such as has been found for the PVM-100, would permit various FSSP-100 flown with the PVM-100A to be compared with each other better than before.

ACKNOWLEDGMENTS

Gabor Vali of the University of Wyoming is thanked for his contribution to the design of the new aircraft probe. We thank Gerard Kos of ECN for his fine effort during the ECN calibration. The help of Jack Russel, Dean Hegg, and Ronald Ferek of the University of Washington, and of Ken McMillan and Rodney Sorrenson, the pilots of the C-131A is much appreciated. This work was supported by NSF Grant ATM-9207345 and NASA P.O. 913-44468.

REFERENCES

Arends, B.B., Kos, G.P.A., Wobrock, W., Schell, D., Noone, K.J., Fuzzi, S. and Pahl, S., 1992. Comparison of techniques for measurements of fog liquid water content. Tellus, 44B: 604-611.

Azzopardi, B.J., 1979. Measurement of drop sizes. Int. J. Heat Mass Transfer, 22: 1245-1279.

Baumgardner, D. and Spowart, M., 1990. Evaluation of forward scattering spectrometer probe. Part III: Time response and laser inhomogeneity limitations. J. Atmos. Oceanic Technol., 7: 666-672.

Baumgardner, D., Strapp, W. and Dye, J.E., 1985. Evaluation of the forward scattering spectrometer probe. Part II: Corrections for coincidence and dead-time losses. J. Atmos. Oceanic Technol., 2: 626-632.

Biter, C.J., Dye, J.E., Huffman, D. and King, W.D., 1987. The drop-size response of the CSIRO liquid water probe. J. Atmos. Oceanic Technol., 4: 359-367.

Blyth, A.M., Chittenden, A.M.I. and Latham, J. 1984: An optical device for the measurement of liquid water content in clouds. Quart. J. Roy. Meteor. Soc., 110: 53-63.

Brenguier, J.L., 1989. Coincidence and dead-time corrections for particle counters. Part II: High concentration measurements with an FSSP. J. Atmos. Oceanic Technol., 6: 585-598.

Brenguier, J.L. and Amodei, L., 1989. Coincidence and dead-time

corrections for particle counters. Part I: A general mathematical formalism. J. Atmos. Oceanic Technol., 6: 575-584.

Breuer, H., 1960. Staubmessungen im Steinkohlenbergbau. Staub, 20: 290-296.

Chylek, P., 1978. Extinction and liquid water content of fogs and clouds. J. Atmos. Sci., 35: 296-300.

Cooper, W.A., 1988: Effects of coincidence on measurements with a forward scattering spectrometer probe. J. Atmos. Oceanic Technol., 5: 823-832.

Gerber, H., 1984. Liquid water content of fogs and hazes from visible light scattering. J. Climate Appl. Meteor., 23: 1247-1252.

Gerber, H., 1991. Direct measurement of suspended particulate volume concentration and far-infrared extinction coefficient with a laser-diffraction instrument. Appl. Opt., 30: 4824-4831.

Gerber, H., 1992. New microphysics sensor for aircraft use. Proc. 11th Intern. Conf. on Clouds and Precipitation, Montreal, 1992: 942-944.

Gertler, A.W. and Steele, R.L., 1980: Experimental verification of the linear relationship between ir extinction and liquid water content of clouds. J. Appl. Meteor., 19: 1314-1317.

Hirleman, E.D., 1984. Particle sizing by optical nonimaging techniques. Liquid Particle Size Measurement Techniques, Tishkoff, J.M., ed., Am. Soc. Test Mater. Spec. Tech. Publ. 848: 39-48.

King, W.D., Dye, J.E., Strapp, J.W., Baumgardner, D. and Huffman, D., 1985. Icing wind tunnel tests on the CSIRO liquid water probe. J. Atmos. Oceanic Technol., 2: 340-352.

King, W.D., Parkin, D.A. and Handsworth, R.J., 1978: Hot-wire water device having fully calculable response characteristics. J. Appl. Meteor., 17: 1809-1813.

Mallant, R.K.A.M., 1988: A fog chamber and wind tunnel facility for calibration of cloud water collectors. Acid Deposition at High Elevation Sites, Unworth, M.H. and Fowler, D., eds., Klumer Academic Pub., The Netherlands: 479-490.

Nolan, P.F. and Jennings, S.G., 1987: Extinction and liquid water content measurements at CO laser wavelengths. J. Atmos. Oceanic Technol., 4: 491-400.

Pinnick, R.G., Jennings, S.G., Chylek, P. and Auverman, H.V., 1979. Verification of a linear relationship between ir extinction, absorption and liquid water content of fogs. J. Atmos. Sci., 36: 1577-1586.

Slingo, A., 1989. A GCM parameterization for the shortwave radiative properites of water clouds. J. Atmos. Sci., 46: 1419-1426.

Slingo, A., 1990. Sensitivity of the Earth's radiation budget to changes in low clouds. Nature, 343: 49-51.

Stetter, G., 1949. Dust inspection by optical measurements. Microtecnic, 3: 234-239.

Strapp, J.W. and Schemenauer, 1982. Calibration of Johnson-Williams liquid water content meters in a high-speed icing tunnel. J. Appl. Meteor., 21: 98-108.

Swithenbank, J., Beer, J.M., Taylor, DE.S., Abbot, D. and McCreath, G.C., 1976. A laser diagnostic for the measurement of droplet and particle size distributions. Prog. Astronaut. Aeronaut., 53: 421-429.

Valente, R.J., Mallant, R.K.A.M., McLaren, S.E., Schemenauer, R.S. and Stogner, R.E., 1989. Field intercomparison of ground-based cloud physics instruments at Whitetop Mountain, Virginia. J. Atmos. Oceanic Technol., 6: 396-406.

Wertheimer, A.L. and Wilcock, W.L., 1976. Light scattering measurements of particle distributions. Appl. Opt., 15: 1616-1620.

FIGURE AND TABLE CAPTIONS

Fig. 1 - Probe of PVM-100A; top view (upper), and rear view (lower). Dimensions in cm.

Fig. 2 - Sketch of main optical components and operating principle of the PVM-100A. Cubic beamsplitter divides scattered light 50%/50%. Filters with concentric regions of

different transmittance weight the scattered light to produce sensor outputs proportional to LWC and PSA.

Fig. 3 - Schematic of fog-wind tunnel at ECN. A (blower), B (water reservoir), C (humidifier), D (fog-droplet generator), E (mixing chamber), F (test section), G (water pump), H (heater) [from Mallant, (1988)].

Fig. 4 - Droplet size spectra generated in the ECN chamber for calibration of the PVM-100A. Numbers refer to volume median diameters (um), VMD, for the spectra.

Fig. 5 - Comparison of LWC measured with the ground-based instrument, PVM-100, and the filter method in the ECN chamber for two VMD. K = 1.05.

Fig. 6 - Comparisons of LWC measured with the FSSP-100, the filter method, and the PVM-100A in the ECN chamber during the calibration of the PVM-100A. A scaling factor of 2.58 is applied to the PVM-100A output voltage to calculate LWC. Numbers indicate test numbers given in Table 1.

Fig. 7 - VMD of droplet spectra measured by the FSSP-100 vs the ratio of FSSP LWC to filter LWC.

Fig. 8 - Comparison of the PVM-100A voltage output for droplet surface area (PSA) and PSA calculated from the FSSP-100 spectra. See text for the significance of the solid-circle and open-circle data.

Fig. 9 - VMD measured by the FSSP-100 (except upper left point)

as a function of the ratio of FSSP LWC to filter LWC. Curve is given by second-order polynomial shown fitted to data.

Fig. 10 - Comparison of LWC measured by the FSSP-100, PVM-100A, JW, and King probes in a broken cloud field traversed by the U. of Washington C-131A aircraft during ASTEX.

Fig. 11 - Comparison of LWC measured by the FSSP-100, PVM-100A, and King probes during a vertical traverse of a marine stratocumulus layer by the C-131A with the calculated adiabatic LWC profile.

Fig. 12 - Effective droplet radius measured by co-located FSSP-100 and PVM-100A on the C-131A (hollow circles). Horizontal bars give a laboratory comparison of droplet diameters measured with FSSP-100 at aircraft speed (horizontal axis) and actual droplet diameters (vertical axis); from Baumgardner and Spowart (1990). Linear regression gives the straight line through the PVM-100A data.

Table 1 - ECN calibration tests of the PVM-100A. Nebulizer types: H = Heyer '77 ultrasonic; L = Lee Instac pneumatic; W = Wagner 220 ultrasonic. (p) denotes low-pressure operation. FSSP correction is for compensating dead-time and coincidence errors, calculated from Baumgardner et al. (1985).

Test No.	Neb. Type	Filter LWC g/m^3	FSSP LWC g/m^3	FSSP PSA cm^2/m^3	FSSP VMD um	FSSP Conc. $no./cm^3$	FSSP Corr.	PVM LWC V	PVM PSA V
1	1H	.1376	.132	800	10.2	452	1.135	.0452	.0985
2	2H	.2038	.224	1210	11.7	496	1.149	.0829	.1710
3	3H	.2899	.282	1390	12.9	456	1.137	.1214	.2285
4	1L	.3022	.407	1520	18.9	427	1.127	.1184	.1600
5	2L	.4952	.692	2330	20.5	490	1.147	.2052	.2685
6	2L(p)	.2743	.491	1260	29.4	249	1.072	.0819	.0835
7	1L(p)	.1438	.281	701	30.1	139	1.040	.0434	.0445
8	3L	.7575	.940	2930	21.5	471	1.141	.2880	.3935
9	1W	.4809	.924	1690	40.6	169	1.049	.0939	.0860
10	1W,3L	.9587	1.510	3720	27.8	468	1.140	.3374	.4260

Table 1

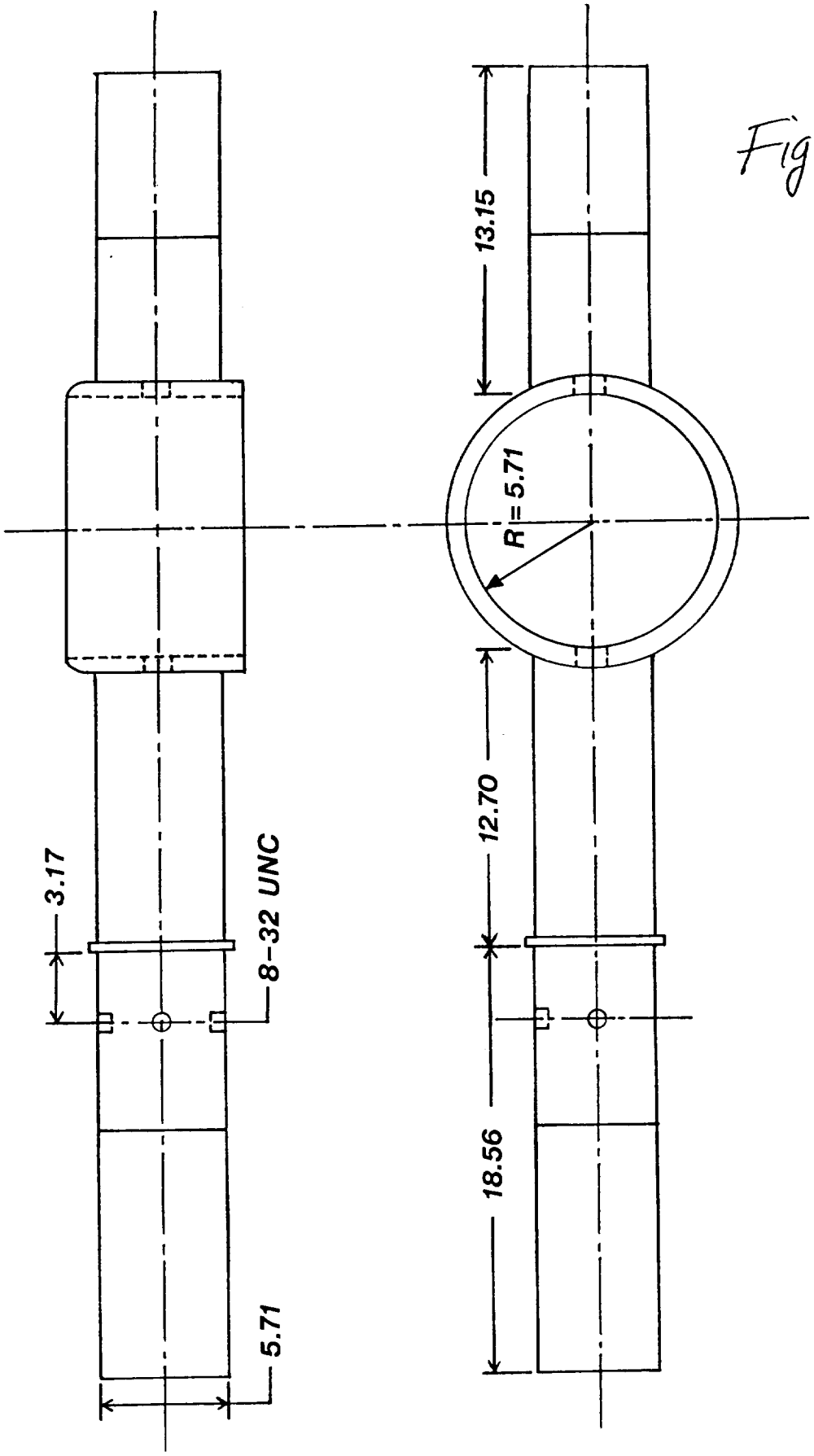

Fig. 1

Fig. 2

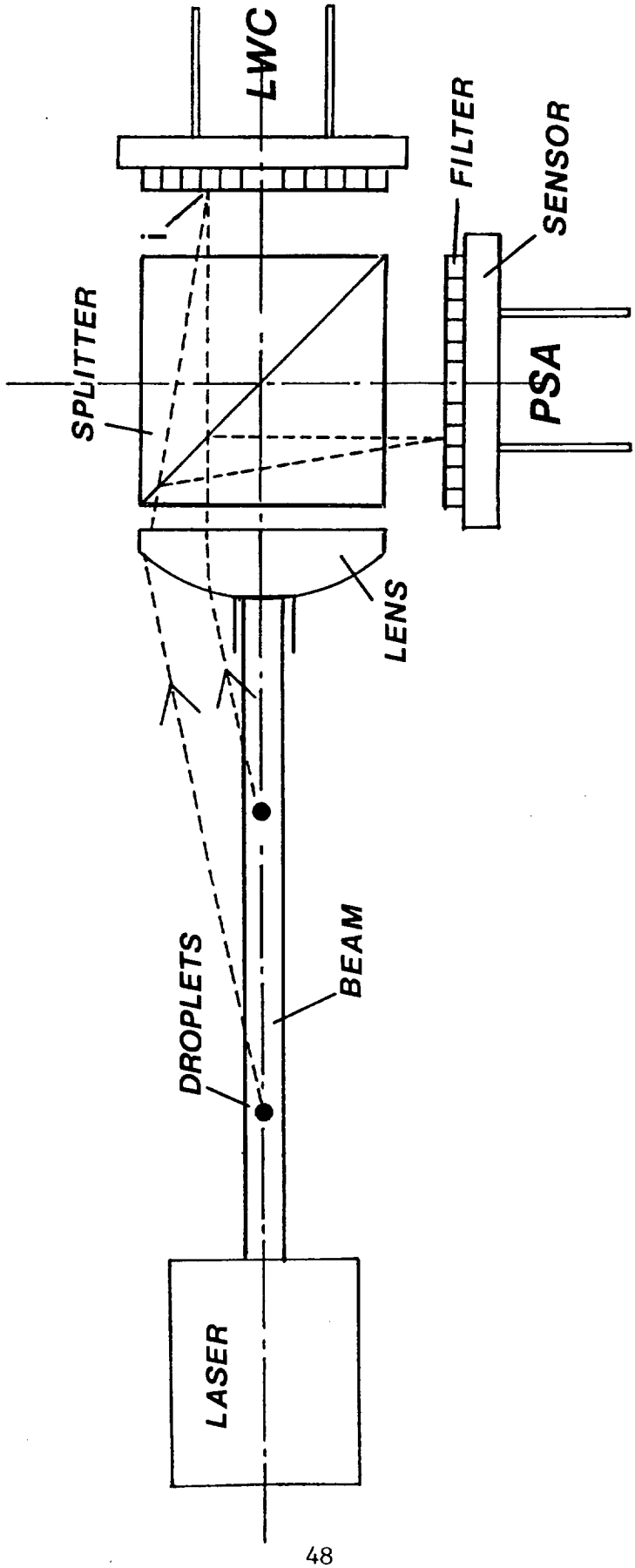

Fig. 3

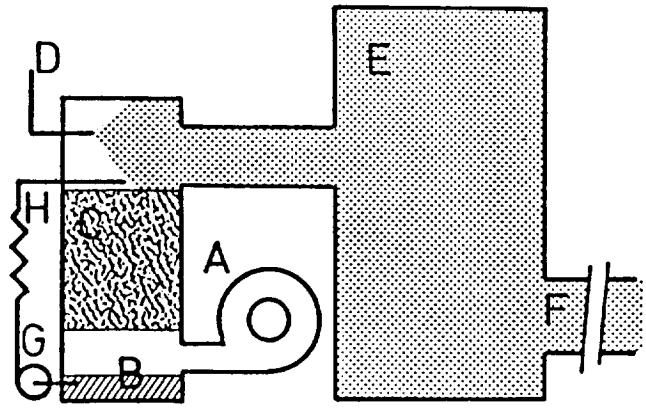

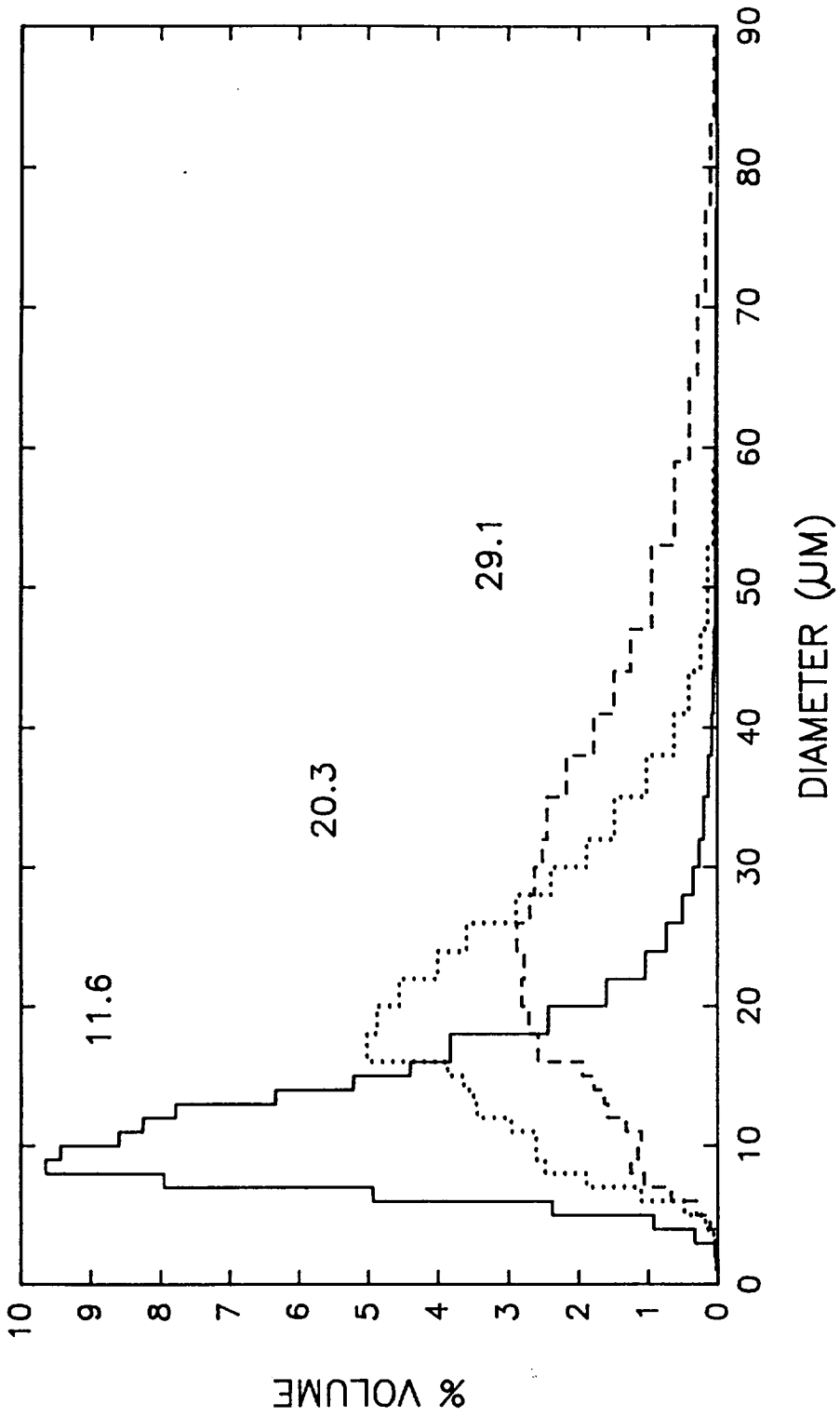
% VOLUME
0
1
2
3
4
5
6
7
8
9
10
DIAMETER (µM)
0
10
20
30
40
50
60
70
80
90
11.6
20.3
29.1

Fig. 4

Fig. 5

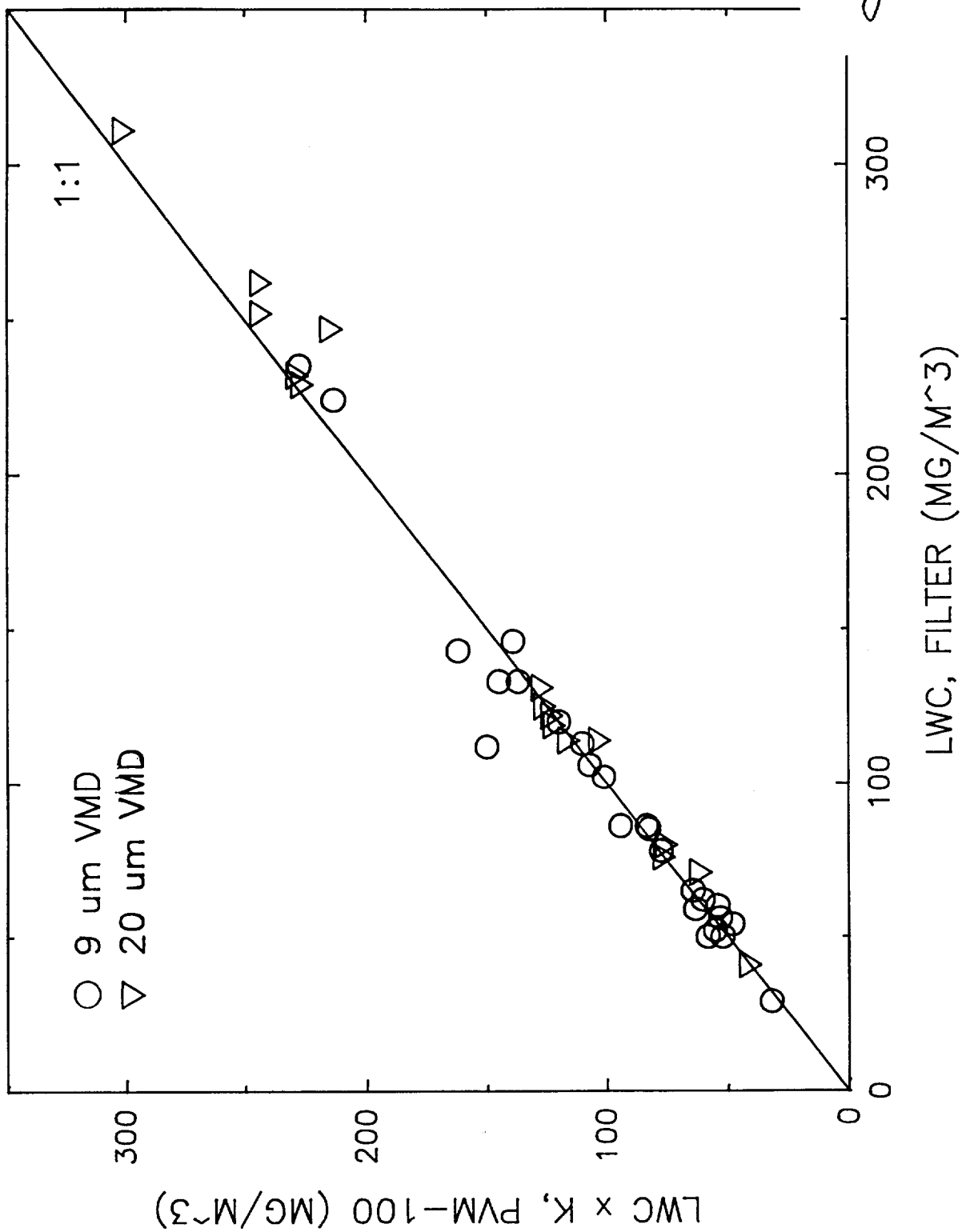
1:1
9 um VMD
20 um VMD
LWC, FILTER (MG/M^3)
LWC x K, PVM-100 (MG/M^3)
0
100
200
300

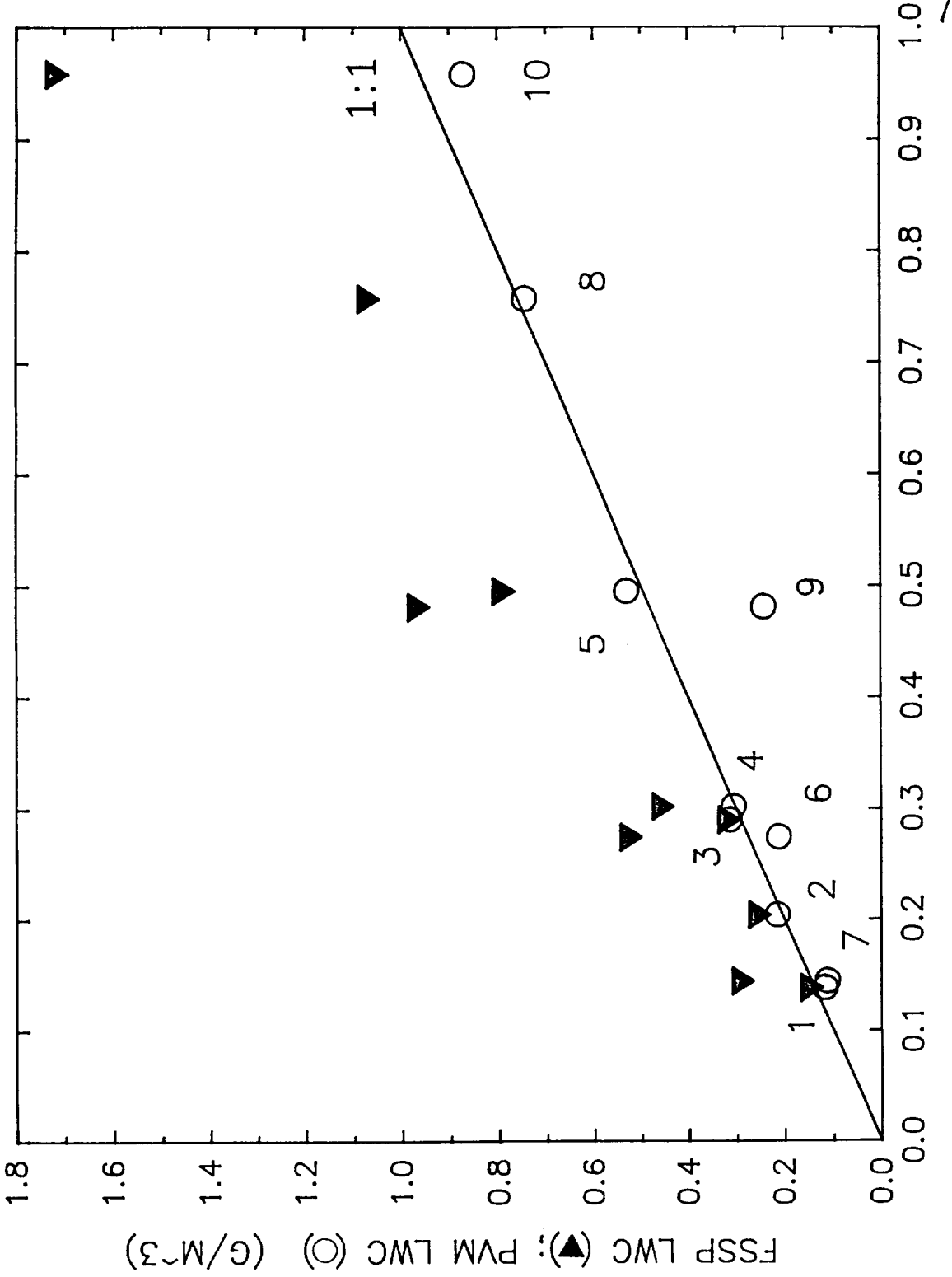
1:1
10
8
5
9
4
6
3
2
7
1
0.0
0.1
0.2
0.3
0.4
0.5
0.6
0.7
0.8
0.9
1.0
FILTER LWC (G/M^3)
0.0
0.2
0.4
0.6
0.8
1.0
1.2
1.4
1.6
1.8
FSSP LWC (▲); PVM LWC (○) (G/M^3)

Fig. 6

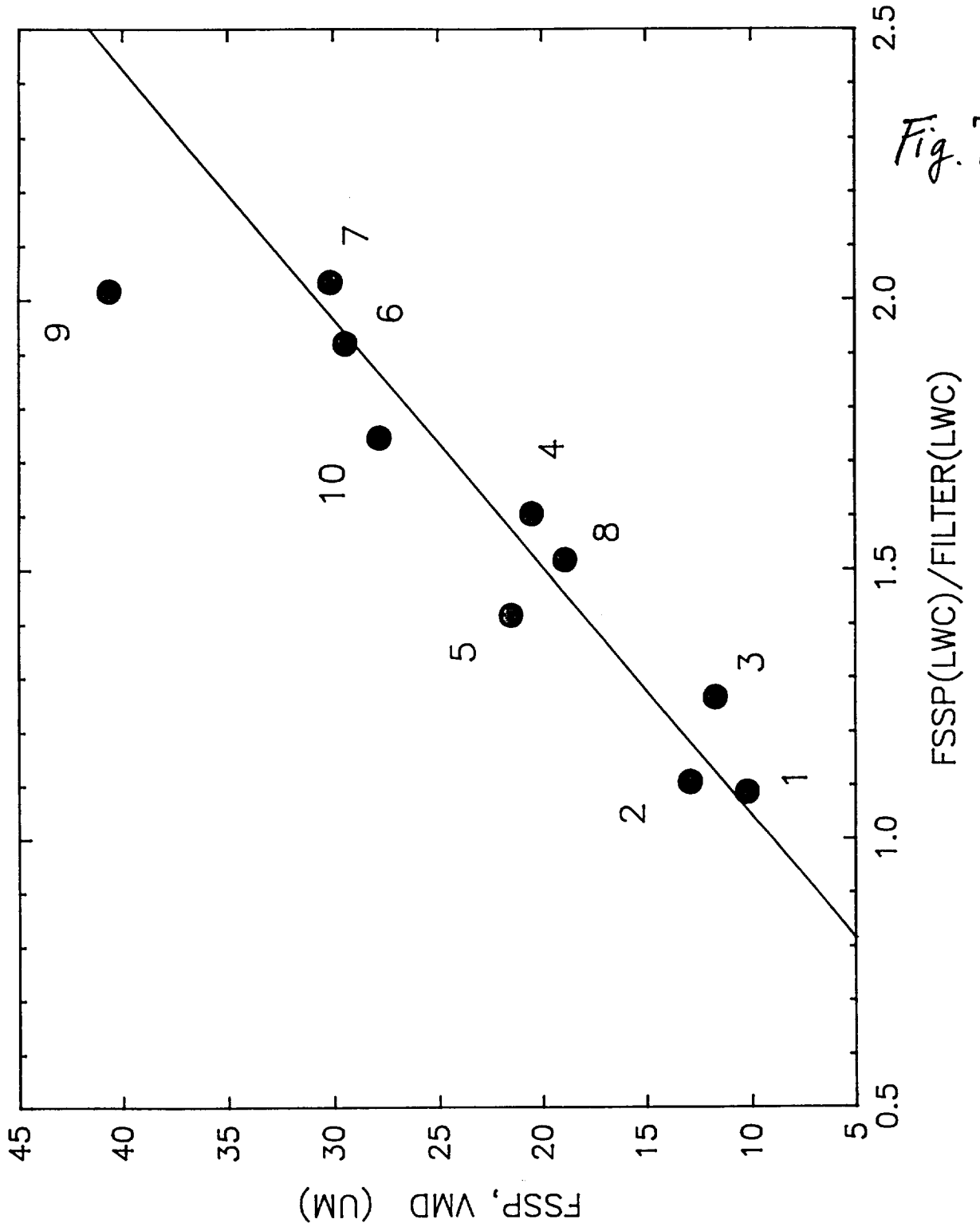
FSSP, VMD (UM)
FSSP(LWC)/FILTER(LWC)
45
40
35
30
25
20
15
10
5
0.5
1.0
1.5
2.0
2.5
1
2
3
4
5
6
7
8
9
10

Fig. 7

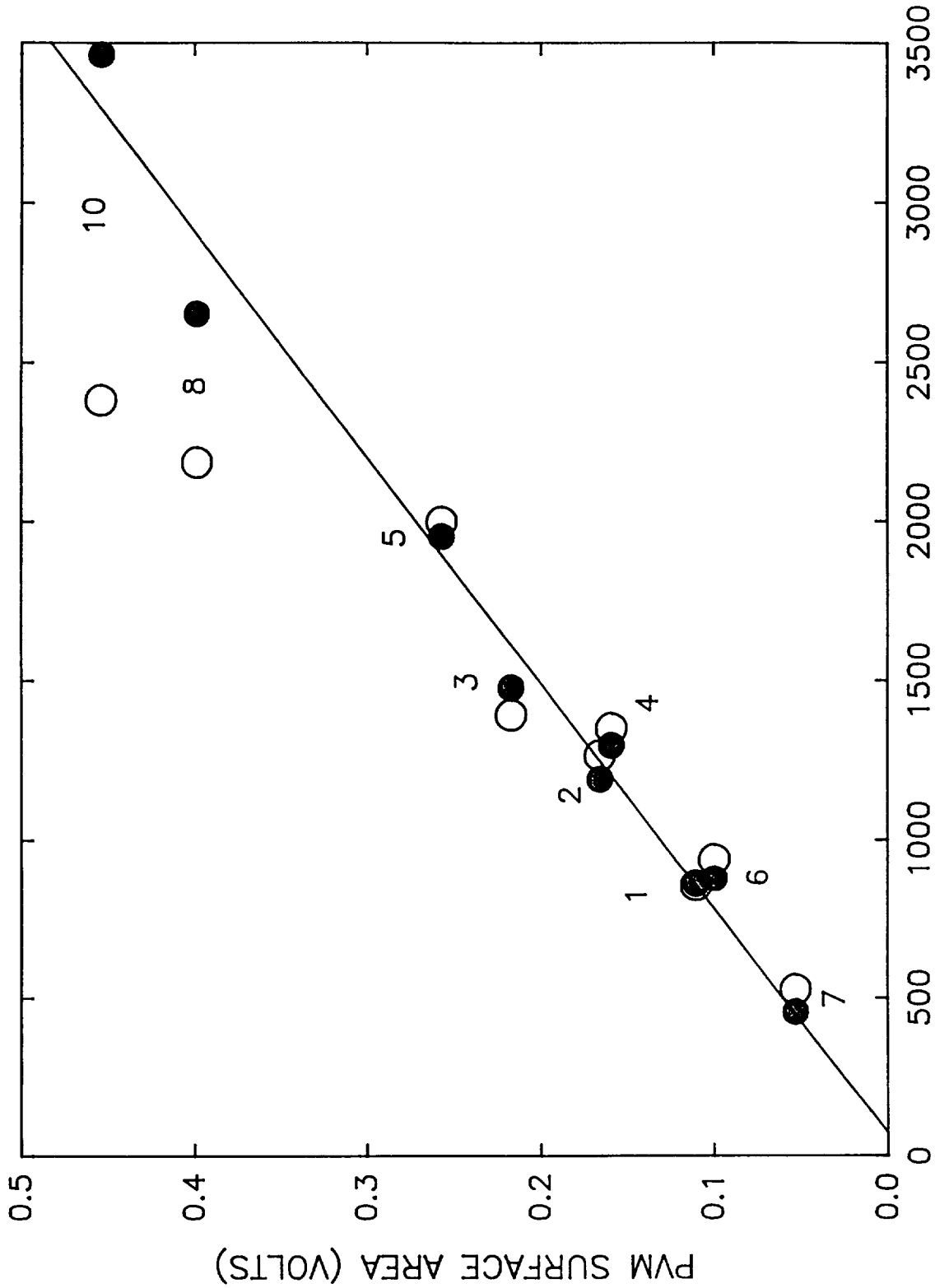
PVM SURFACE AREA (VOLTS)
0.0
0.1
0.2
0.3
0.4
0.5
FSSP SURFACE AREA (CM^2/M^3)
0
500
1000
1500
2000
2500
3000
3500
1
2
3
4
5
6
7
8
10

Fig. 8

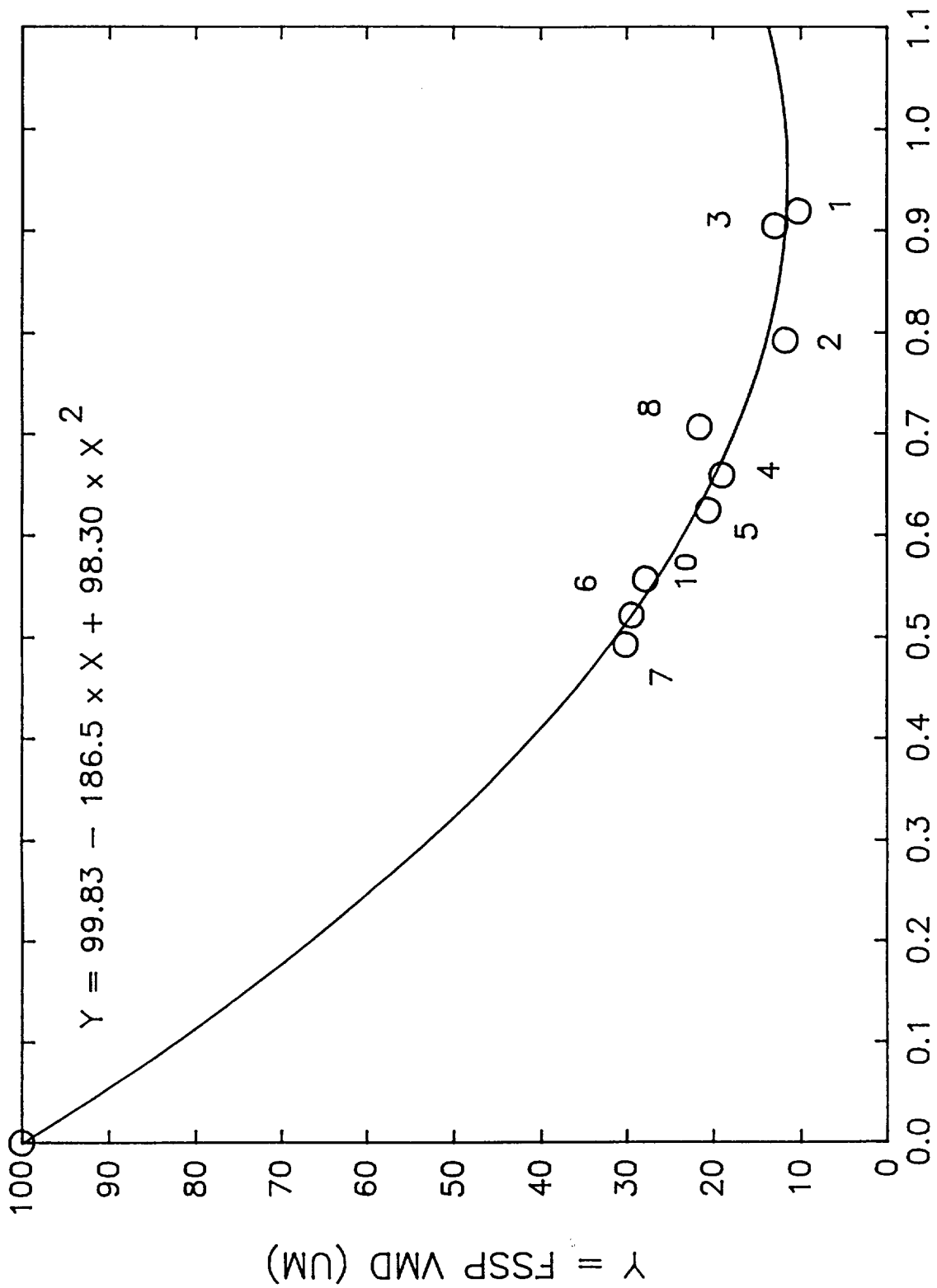
Y = 99.83 − 186.5 × X + 98.30 × X 2
Y = FSSP VMD (UM)
X = FILTER LWC/FSSP LWC
100
90
80
70
60
50
40
30
20
10
0
0.0
0.1
0.2
0.3
0.4
0.5
0.6
0.7
0.8
0.9
1.0
1.1
1
2
3
4
5
6
7
8
10

Fig. 9

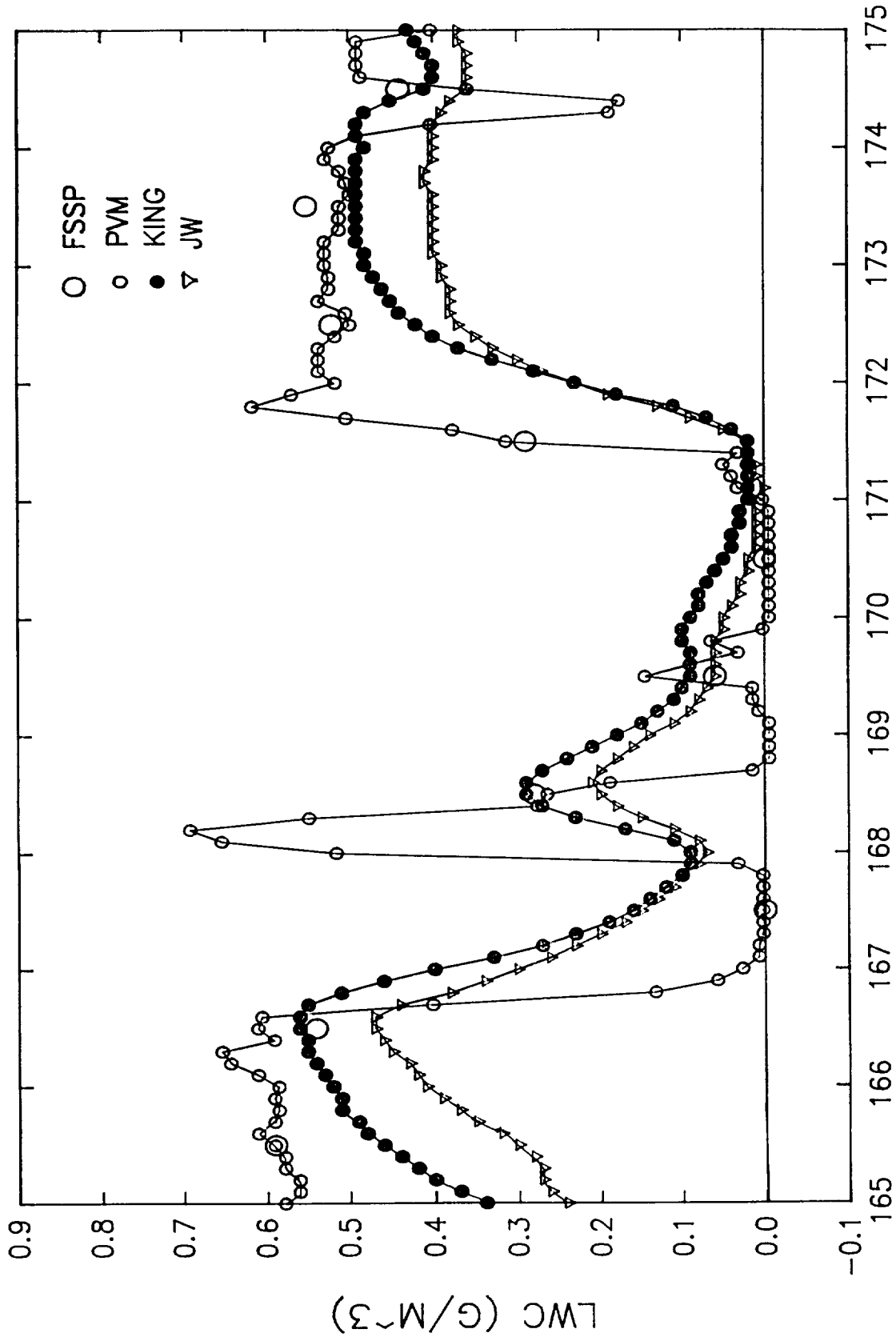
FSSP
PVM
KING
JW
LWC (G/M^3)
TIME (SEC)
0.9
0.8
0.7
0.6
0.5
0.4
0.3
0.2
0.1
0.0
-0.1
165
166
167
168
169
170
171
172
173
174
175

Fig. 10

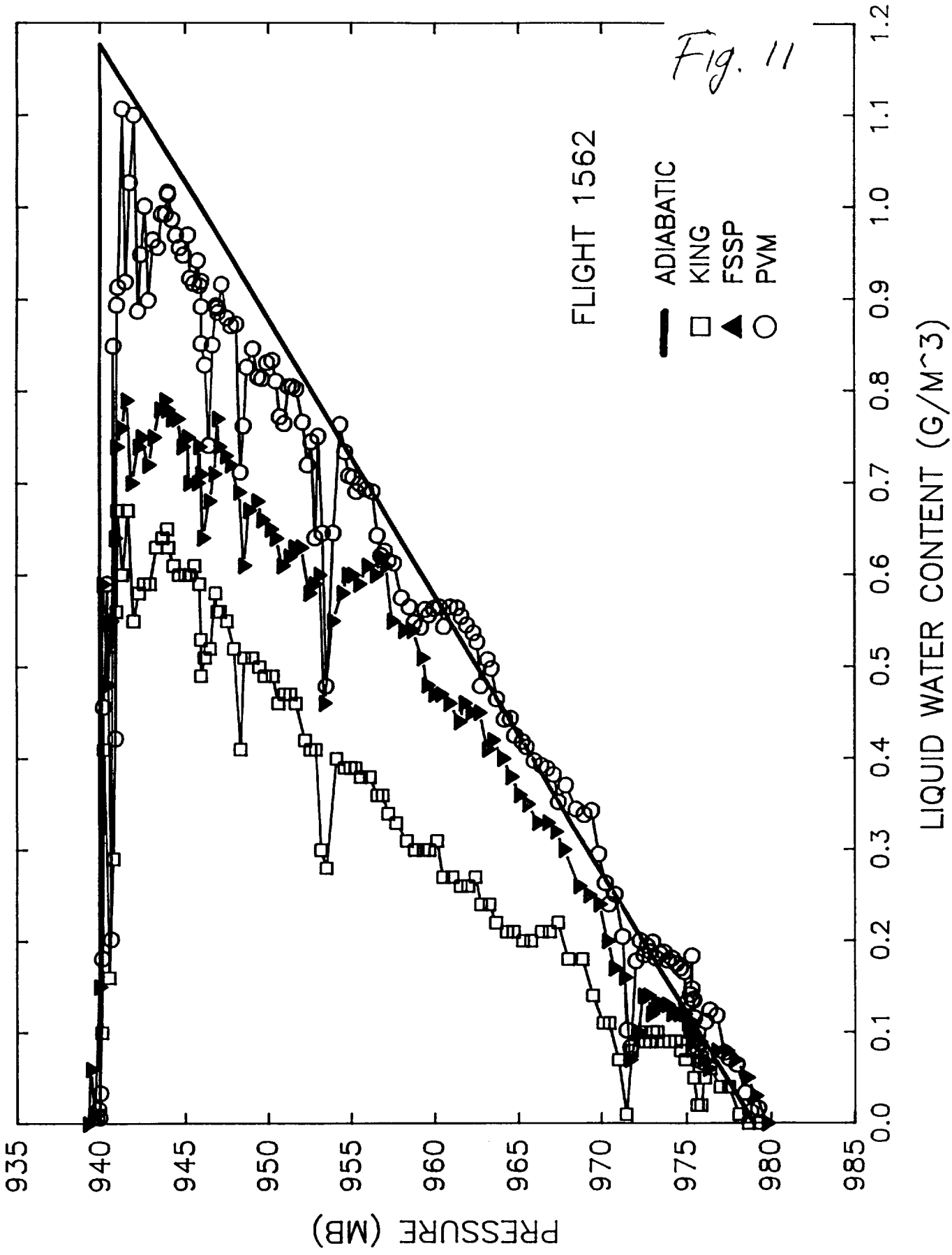
FLIGHT 1562
ADIABATIC
KING
FSSP
PVM
PRESSURE (MB)
935
940
945
950
955
960
965
970
975
980
985
LIQUID WATER CONTENT (G/M^3)
0.0
0.1
0.2
0.3
0.4
0.5
0.6
0.7
0.8
0.9
1.0
1.1
1.2

Fig. 11

Fig. 12

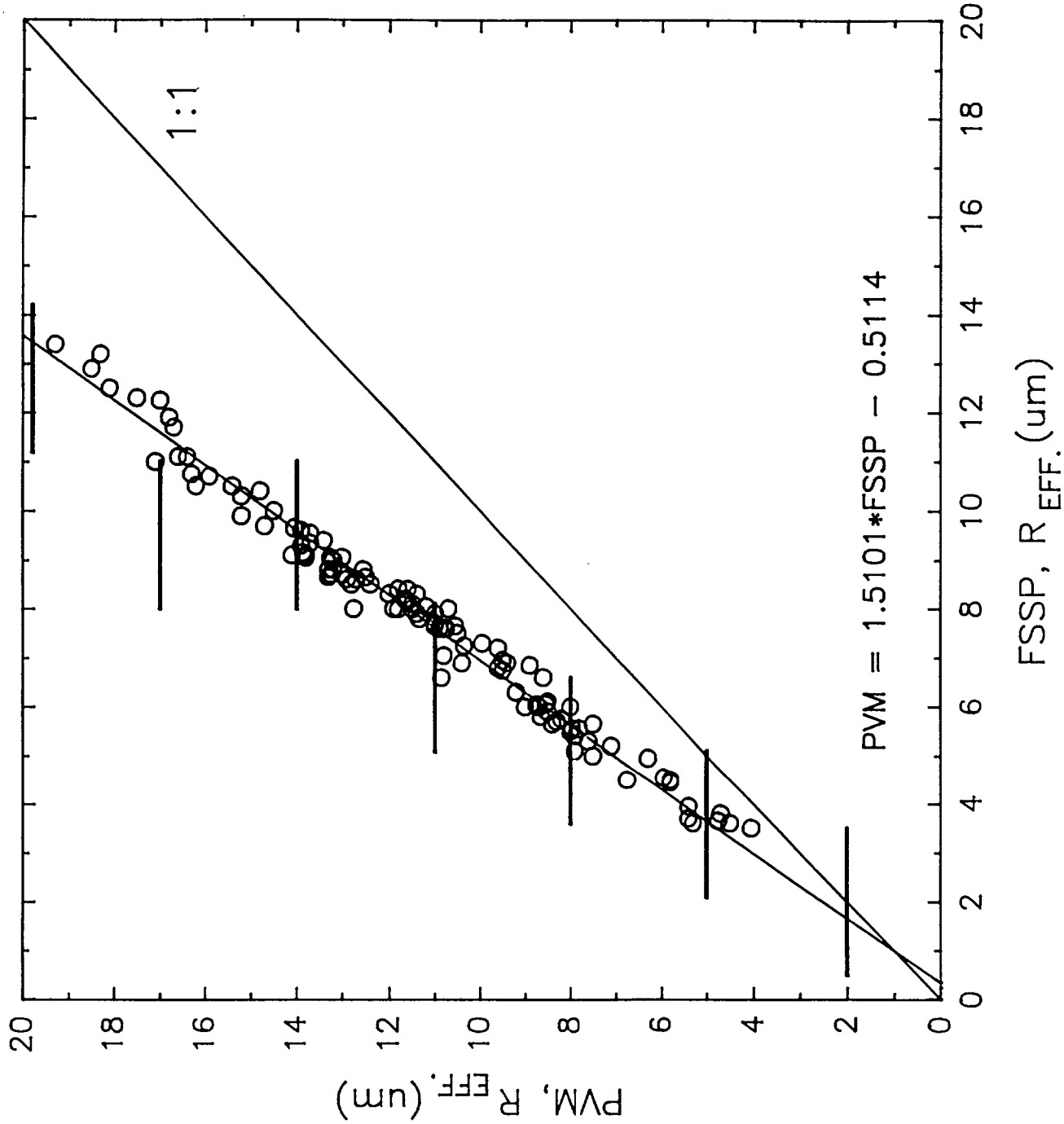
1:1
PVM = 1.5101*FSSP − 0.5114
PVM, R EFF. (um)
FSSP, R EFF. (um)
0
2
4
6
8
10
12
14
16
18
20

APPENDIX C

Notes:

1) On pg. 60 the following definitions apply:
   SSFSSP95 = 100 x LWC(g/m^3) for FSSP-100
   surface = 0.1 x PSA(cm^2/m^3) for FSSP-100
2) Units given in the following pages for SURFACE and VOLUME distributions measured with the FSSP-100 are incorrect. They should read, respectively um^2/cm^2, and um^3/cm^3 ,um.

Summarized data

Summary of the results of the LWC-comparison-measurements and LWC - surface measurements on march 17 thru 19, 1992.

CHIEF at a flowrate of 31 m^3/min. air speed 2.15 m/s

Ultra sonic nebulizers, Lee150k nebulizers, "paintspray-nebulizer".

Temperature about 23 degrees centigrade.

Used instruments: FSSP95 and PVM100A.

Two filterreference-measurements (samples sucked isokinetically) in all tests.

Table LWC in mg/m^3

	Run ---------->>									
Descr.	1.0	2.0	3.0	4.0	5.0	6.0	7.0	8.0	9.0	10
Generated	N.A.	242.8	283.2	387.7	777.0	750.0	384.8	1056.0	N.A.	N.
FilterI	140.0	204.7	293.4	306.3	495.6	269.8	146.4	765.3	495.2	975
FilterII	135.2	202.9	286.4	297.7	494.7	278.8	141.1	749.7	466.2	941
AVG Filt	137.6	203.8	289.9	302.2	495.2	274.3	143.8	757.5	480.9	958
PDSFSSP	115.0	198.0	254.0	384.3	662.0	469.3	271.5	907.0	903.0	1467
SSFSSP95	132.0	224.0	282.0	407.0	692.0	491.0	281.0	940.0	924.0	1510
surface ($um^2/m^3/dD$)	80.0	121.0	139.0	152.0	233.0	126.0	70.1	293.0	169.0	372
FSHOWFP95	132.0	224.0	282.0	407.0	692.0	491.0	281.0	940.0	924.0	1510
PVM100A (mVolts)	53.0	90.7	129.2	126.2	213.0	89.7	51.2	295.8	101.7	345
std	1.2	1.4	2.5	1.1	1.6	10.5	1.3	2.8	1.8	3

FSSP95-spectra

Date : march 17 1992 distribution: NUMBER

period: Run 1

diam. interval

upper-limit (um)	lower-limit (um)	Raw Counts	aantal n/cc /um	aantal n/cc/ interval	aantal in %	aantal accum. %
1	2	41882,17	20,52	20,52	4,57	4,6
2	3	29423,00	14,42	14,42	3,21	7,8
3	4	74767,17	36,63	36,63	8,16	15,9
4	5	92233,83	45,19	45,19	10,07	26,0
5	6	125452,33	61,47	61,47	13,69	39,7
6	7	148704,33	72,86	72,86	16,23	55,9
7	8	143878,33	70,50	70,50	15,70	71,6
8	9	103744,33	50,83	50,83	11,32	83,0
9	10	60055,67	29,43	29,43	6,55	89,5
10	11	33626,50	16,48	16,48	3,67	93,2
11	12	22288,17	10,92	10,92	2,43	95,6
12	13	15213,83	7,45	7,45	1,66	97,3
13	14	9095,00	4,46	4,46	0,99	98,3
14	15	5877,50	2,88	2,88	0,64	98,9
15	16	4183,83	2,05	2,05	0,46	99,4
16	18	5627,67	1,38	2,76	0,31	99,7
18	20	2745,17	0,67	1,35	0,15	99,8
20	22	1435,17	0,35	0,70	0,08	99,9
22	24	783,83	0,19	0,38	0,04	99,9
24	26	467,33	0,11	0,23	0,03	100,0
26	28	273,33	0,07	0,13	0,01	100,0
28	30	172,00	0,04	0,08	0,01	100,0
30	32	109,33	0,03	0,05	0,01	100,0
32	35	100,50	0,02	0,05	0,00	100,0
35	38	61,50	0,01	0,03	0,00	100,0
38	41	31,33	0,01	0,02	0,00	100,0
41	44	18,00	0,00	0,01	0,00	100,0
44	47	10,00	0,00	0,00	0,00	100,0
47	53	11,67	0,00	0,01	0,00	100,0
53	59	7,67	0,00	0,00	0,00	100,0
59	65	4,33	0,00	0,00	0,00	100,0
65	71	1,33	0,00	0,00	0,00	100,0
71	77	2,33	0,00	0,00	0,00	100,0
77	83	0,33	0,00	0,00	0,00	100,0
83	89	0,33	0,00	0,00	0,00	100,0
89	95	0,33	0,00	0,00	0,00	100.0
95						
totaal		922289		452	100	

Date : march 17 1992 distribution: SURFACE

period: Run 1

diam. interval

upper-limit (um)	lower-limit (um)	surface um^2/m^3 /um	surface um^2/m^3 interval	surface in %	surface accum. %
1	2	150	150	0,2	0,2
2	3	287	287	0,4	0,5
3	4	1419	1419	1,8	2,3
4	5	2887	2887	3,6	5,9
5	6	5858	5858	7,3	13,3
6	7	9690	9690	12,1	25,4
7	8	12476	12476	15,6	41,0
8	9	11551	11551	14,4	55,4
9	10	8351	8351	10,4	65,9
10	11	5711	5711	7,1	73,0
11	12	4540	4540	5,7	78,7
12	13	3661	3661	4,6	83,2
13	14	2553	2553	3,2	86,4
14	15	1903	1903	2,4	88,8
15	16	1548	1548	1,9	90,8
16	18	1253	2506	3,1	93,9
18	20	763	1527	1,9	95,8
20	22	487	975	1,2	97,0
22	24	319	639	0,8	97,8
24	26	225	450	0,6	98,4
26	28	153	307	0,4	98,8
28	30	111	223	0,3	99,0
30	32	81	162	0,2	99,2
32	35	58	174	0,2	99,5
35	38	42	126	0,2	99,6
38	41	25	75	0,1	99,7
41	44	17	50	0,1	99,8
44	47	11	32	0,0	99,8
47	53	7	45	0,1	99,9
53	59	6	37	0,0	99,9
59	65	4	26	0,0	99,9
65	71	2	9	0,0	100,0
71	77	3	20	0,0	100,0
77	83	1	3	0,0	100,0
83	89	1	4	0,0	100,0
89	95	1	4	0,0	100,0
95					
totaal			8,00E+4	100,00	

Date : march 17 1992 distribution: VOLUME

period: Run 1

diam. interval

lower-limit (um)	upper-limit (um)	volume um^3/m^3 /um	volume um^3/m^3 interval	volume in %	volume accum %	mass(*) mg/m^3/ interval
1	2	40	40	0,0	0,0	0,04
2	3	123	123	0,1	0,1	0,12
3	4	839	839	0,6	0,8	0,84
4	5	2183	2183	1,6	2,4	2,18
5	6	5399	5399	4,1	6,5	5,40
6	7	10539	10539	8,0	14,4	10,54
7	8	15642	15642	11,8	26,2	15,64
8	9	16402	16402	12,4	38,6	16,40
9	10	13246	13246	10,0	48,6	13,25
10	11	10009	10009	7,6	56,2	10,01
11	12	8713	8713	6,6	62,8	8,71
12	13	7635	7635	5,8	68,5	7,64
13	14	5749	5749	4,3	72,9	5,75
14	15	4602	4602	3,5	76,3	4,60
15	16	4001	4001	3,0	79,4	4,00
16	18	3559	7118	5,4	84,7	7,12
18	20	2422	4844	3,7	88,4	4,84
20	22	1709	3418	2,6	91,0	3,42
22	24	1226	2451	1,9	92,8	2,45
24	26	938	1876	1,4	94,2	1,88
26	28	691	1382	1,0	95,3	1,38
28	30	539	1077	0,8	96,1	1,08
30	32	418	836	0,6	96,7	0,84
32	35	324	971	0,7	97,5	0,97
35	38	256	769	0,6	98,0	0,77
38	41	165	496	0,4	98,4	0,50
41	44	118	355	0,3	98,7	0,35
44	47	81	242	0,2	98,9	0,24
47	53	63	375	0,3	99,1	0,38
53	59	58	346	0,3	99,4	0,35
59	65	44	266	0,2	99,6	0,27
65	71	18	108	0,1	99,7	0,11
71	77	40	243	0,2	99,9	0,24
77	83	7	44	0,0	99,9	0,04
83	89	9	54	0,0	99,9	0,05
89	95	11	67	0,1	100,0	0,07
95						
totaal			1,32E+5	100,00		132

*) If Rho = 1.0

Date : march 17 1992 distribution: NUMBER

period: Run 2

diam. interval

upper-limit (um)	lower-limit (um)	Raw Counts	aantal n/cc /um	aantal n/cc/ interval	aantal in %	aantal accum. %
1	2	17136,33	8,40	8,40	1,71	1,7
2	3	18629,67	9,13	9,13	1,86	3,6
3	4	48602,33	23,81	23,81	4,86	8,4
4	5	68311,67	33,47	33,47	6,83	15,3
5	6	101071,00	49,52	49,52	10,11	25,4
6	7	135787,00	66,53	66,53	13,58	39,0
7	8	151529,33	74,25	74,25	15,16	54,1
8	9	136753,00	67,01	67,01	13,68	67,8
9	10	101934,33	49,95	49,95	10,20	78,0
10	11	70923,33	34,75	34,75	7,09	85,1
11	12	51025,67	25,00	25,00	5,10	90,2
12	13	36623,33	17,94	17,94	3,66	93,9
13	14	23291,33	11,41	11,41	2,33	96,2
14	15	15061,33	7,38	7,38	1,51	97,7
15	16	10215,33	5,01	5,01	1,02	98,7
16	18	13353,67	3,27	6,54	0,67	99,4
18	20	6077,67	1,49	2,98	0,30	99,7
20	22	2926,33	0,72	1,43	0,15	99,8
22	24	1394,33	0,34	0,68	0,07	99,9
24	26	765,00	0,19	0,37	0,04	100,0
26	28	411,67	0,10	0,20	0,02	100,0
28	30	235,00	0,06	0,12	0,01	100,0
30	32	141,33	0,03	0,07	0,01	100,0
32	35	128,33	0,02	0,06	0,00	100,0
35	38	51,67	0,01	0,03	0,00	100,0
38	41	27,33	0,00	0,01	0,00	100,0
41	44	17,33	0,00	0,01	0,00	100,0
44	47	12,00	0,00	0,01	0,00	100,0
47	53	10,67	0,00	0,01	0,00	100,0
53	59	5,33	0,00	0,00	0,00	100,0
59	65	3,33	0,00	0,00	0,00	100,0
65	71	2,33	0,00	0,00	0,00	100,0
71	77	2,67	0,00	0,00	0,00	100,0
77	83	0,00	0,00	0,00	0,00	100,0
83	89	1,00	0,00	0,00	0,00	100,0
89	95	0,67	0,00	0,00	0,00	100,0
95						
totaal		1012463		496	100,00	

Date : march 17 1992 distribution: SURFACE

period: Run 2

diam. interval

upper-limit (um)	lower-limit (um)	surface um^2/m^3 /um	surface um^2/m^3 interval	surface in %	surface accum. %
1	2	62	62	0,1	0,1
2	3	182	182	0,2	0,2
3	4	923	923	0,8	1,0
4	5	2138	2138	1,8	2,7
5	6	4719	4719	3,9	6,7
6	7	8848	8848	7,3	14,0
7	8	13140	13140	10,9	24,9
8	9	15227	15227	12,6	37,5
9	10	14174	14174	11,7	49,2
10	11	12045	12045	10,0	59,2
11	12	10394	10394	8,6	67,8
12	13	8813	8813	7,3	75,1
13	14	6537	6537	5,4	80,6
14	15	4876	4876	4,0	84,6
15	16	3779	3779	3,1	87,7
16	18	2974	5947	4,9	92,7
18	20	1690	3380	2,8	95,5
20	22	994	1988	1,6	97,1
22	24	568	1136	0,9	98,1
24	26	368	736	0,6	98,7
26	28	231	462	0,4	99,1
28	30	152	304	0,3	99,3
30	32	105	209	0,2	99,5
32	35	74	222	0,2	99,7
35	38	35	106	0,1	99,8
38	41	22	66	0,1	99,8
41	44	16	48	0,0	99,8
44	47	13	38	0,0	99,9
47	53	7	41	0,0	99,9
53	59	4	26	0,0	99,9
59	65	3	20	0,0	100,0
65	71	3	17	0,0	100,0
71	77	4	22	0,0	100,0
77	83	0	0	0	100,0
83	89	2	11	0,0	100,0
89	95	1	9	0,0	100,0
95					
totaal			1,21E+5	100,00	

Date : march 17 1992 distribution: VOLUME

period: Run 2

diam. interval

lower-limit (um)	upper-limit (um)	volume um^3/m^3 /um	volume um^3/m^3 interval	volume in %	volume accum %	mass(*) mg/m^3/ interval
1	2	16	16	0,0	0,0	0,02
2	3	78	78	0,0	0,0	0,08
3	4	546	546	0,2	0,3	0,55
4	5	1617	1617	0,7	1,0	1,62
5	6	4350	4350	1,9	3,0	4,35
6	7	9624	9624	4,3	7,3	9,62
7	8	16473	16473	7,4	14,6	16,47
8	9	21621	21621	9,7	24,3	21,62
9	10	22484	22484	10,1	34,3	22,48
10	11	21111	21111	9,4	43,8	21,11
11	12	19947	19947	8,9	52,7	19,95
12	13	18380	18380	8,2	60,9	18,38
13	14	14722	14722	6,6	67,5	14,72
14	15	11794	11794	5,3	72,8	11,79
15	16	9770	9770	4,4	77,1	9,77
16	18	8445	16890	7,6	84,7	16,89
18	20	5362	10724	4,8	89,5	10,72
20	22	3484	6969	3,1	92,6	6,97
22	24	2180	4361	1,9	94,5	4,36
24	26	1536	3071	1,4	95,9	3,07
26	28	1041	2082	0,9	96,8	2,08
28	30	736	1472	0,7	97,5	1,47
30	32	541	1081	0,5	98,0	1,08
32	35	413	1240	0,6	98,5	1,24
35	38	215	646	0,3	98,8	0,65
38	41	144	433	0,2	99,0	0,43
41	44	114	342	0,2	99,2	0,34
44	47	97	290	0,1	99,3	0,29
47	53	57	343	0,2	99,5	0,34
53	59	40	241	0,1	99,6	0,24
59	65	34	204	0,1	99,7	0,20
65	71	31	189	0,1	99,7	0,19
71	77	46	278	0,1	99,9	0,28
77	83	0	0	0	99,9	0
83	89	27	163	0,1	99,9	0,16
89	95	22	133	0,1	100,0	0,13
95						
totaal			2,24E+5	100,00		224

*) If Rho = 1.0

Date : march 18 1992 distribution: NUMBER

period: Run 3

diam. interval

upper-limit (um)	lower-limit (um)	Raw Counts	aantal n/cc /um	aantal n/cc/ interval	aantal in %	aantal accum. %
1	2	7555,00	3,70	3,70	0,83	0,8
2	3	11181,67	5,48	5,48	1,23	2,1
3	4	29463,00	14,44	14,44	3,24	5,3
4	5	44564,00	21,84	21,84	4,89	10,2
5	6	69156,33	33,88	33,88	7,59	17,8
6	7	99119,00	48,57	48,57	10,89	28,7
7	8	120022,00	58,81	58,81	13,18	41,8
8	9	122183,00	59,87	59,87	13,42	55,3
9	10	105150,33	51,52	51,52	11,55	66,8
10	11	83409,00	40,87	40,87	9,16	76,0
11	12	67111,67	32,88	32,88	7,37	83,3
12	13	52797,00	25,87	25,87	5,80	89,1
13	14	36271,67	17,77	17,77	3,98	93,1
14	15	24852,00	12,18	12,18	2,73	95,9
15	16	17217,00	8,44	8,44	1,89	97,7
16	18	22081,67	5,41	10,82	1,21	99,0
18	20	9833,67	2,41	4,82	0,54	99,5
20	22	4570,67	1,12	2,24	0,25	99,8
22	24	2163,33	0,53	1,06	0,12	99,9
24	26	1141,67	0,28	0,56	0,06	99,9
26	28	562,33	0,14	0,28	0,03	100,0
28	30	290,33	0,07	0,14	0,02	100,0
30	32	169,00	0,04	0,08	0,01	100,0
32	35	154,00	0,03	0,08	0,01	100,0
35	38	70,33	0,01	0,03	0,00	100,0
38	41	32,67	0,01	0,02	0,00	100,0
41	44	16,67	0,00	0,01	0,00	100,0
44	47	12,00	0,00	0,01	0,00	100,0
47	53	14,67	0,00	0,01	0,00	100,0
53	59	8,00	0,00	0,00	0,00	100,0
59	65	5,67	0,00	0,00	0,00	100,0
65	71	2,33	0,00	0,00	0,00	100,0
71	77	1,67	0,00	0,00	0,00	100,0
77	83	1,00	0,00	0,00	0,00	100,0
83	89	0,33	0,00	0,00	0,00	100,0
89	95	0,33	0,00	0,00	0,00	100.0
95						
totaal		931185		456	100	

Date : march 18 1992 distribution: SURFACE

period: Run 3

diam. interval

upper-limit (um)	lower-limit (um)	surface um^2/m^3 /um	surface um^2/m^3 interval	surface in %	surface accum. %
1	2	27	27	0,0	0,0
2	3	109	109	0,1	0,1
3	4	559	559	0,4	0,5
4	5	1395	1395	1,0	1,5
5	6	3229	3229	2,3	3,8
6	7	6459	6459	4,7	8,5
7	8	10408	10408	7,5	16,0
8	9	13604	13604	9,8	25,8
9	10	14621	14621	10,5	36,3
10	11	14166	14166	10,2	46,5
11	12	13671	13671	9,8	56,4
12	13	12705	12705	9,2	65,5
13	14	10180	10180	7,3	72,8
14	15	8046	8046	5,8	78,6
15	16	6369	6369	4,6	83,2
16	18	4917	9835	7,1	90,3
18	20	2735	5470	3,9	94,3
20	22	1553	3105	2,2	96,5
22	24	881	1763	1,3	97,8
24	26	549	1099	0,8	98,6
26	28	316	631	0,5	99,0
28	30	188	376	0,3	99,3
30	32	125	250	0,2	99,5
32	35	89	266	0,2	99,7
35	38	48	144	0,1	99,8
38	41	26	78	0,1	99,8
41	44	15	46	0,0	99,8
44	47	13	38	0,0	99,9
47	53	9	57	0,0	99,9
53	59	6	39	0,0	99,9
59	65	6	34	0,0	100,0
65	71	3	17	0,0	100,0
71	77	2	14	0,0	100,0
77	83	2	10	0,0	100,0
83	89	1	4	0,0	100,0
89	95	1	4	0,0	100,0
95					
totaal			1,39E+5	100,00	

Date : march 18 1992 distribution: VOLUME

period: Run 3

diam. interval

lower-limit (um)	upper-limit (um)	volume um^3/m^3 /um	volume um^3/m^3 interval	volume in %	volume accum %	mass(*) mg/m^3/ interval
1	2	7	7	0,0	0,0	0,01
2	3	47	47	0,0	0,0	0,05
3	4	331	331	0,1	0,1	0,33
4	5	1055	1055	0,4	0,5	1,05
5	6	2976	2976	1,1	1,6	2,98
6	7	7025	7025	2,5	4,1	7,02
7	8	13048	13048	4,6	8,7	13,05
8	9	19317	19317	6,8	15,5	19,32
9	10	23193	23193	8,2	23,7	23,19
10	11	24828	24828	8,8	32,5	24,83
11	12	26235	26235	9,3	41,8	26,24
12	13	26498	26498	9,4	51,2	26,50
13	14	22927	22927	8,1	59,4	22,93
14	15	19461	19461	6,9	66,3	19,46
15	16	16466	16466	5,8	72,1	16,47
16	18	13964	27929	9,9	82,0	27,93
18	20	8676	17352	6,1	88,1	17,35
20	22	5442	10884	3,9	92,0	10,88
22	24	3383	6766	2,4	94,4	6,77
24	26	2292	4584	1,6	96,0	4,58
26	28	1422	2844	1,0	97,0	2,84
28	30	909	1819	0,6	97,7	1,82
30	32	646	1293	0,5	98,1	1,29
32	35	496	1488	0,5	98,6	1,49
35	38	293	879	0,3	99,0	0,88
38	41	172	517	0,2	99,1	0,52
41	44	110	329	0,1	99,3	0,33
44	47	97	290	0,1	99,4	0,29
47	53	79	472	0,2	99,5	0,47
53	59	60	361	0,1	99,7	0,36
59	65	58	347	0,1	99,8	0,35
65	71	31	189	0,1	99,8	0,19
71	77	29	174	0,1	99,9	0,17
77	83	22	132	0,0	100,0	0,13
83	89	9	54	0,0	100,0	0,05
89	95	11	67	0,0	100,0	0,07
95						
totaal			2,82E+5	100,00		282

*) If Rho = 1.0

Date : march 18 1992 distribution: NUMBER

period: Run 4

diam. interval

upper-limit (um)	lower-limit (um)	Raw Counts	aantal n/cc /um	aantal n/cc/ interval	aantal in %	aantal accum. %
1	2	30633,33	15,01	15,01	3,73	3,7
2	3	18470,67	9,05	9,05	2,25	6,0
3	4	45372,33	22,23	22,23	5,52	11,5
4	5	55269,00	27,08	27,08	6,72	18,2
5	6	78907,33	38,66	38,66	9,60	27,8
6	7	104894,00	51,40	51,40	12,76	40,6
7	8	111523,67	54,64	54,64	13,56	54,1
8	9	93153,33	45,64	45,64	11,33	65,5
9	10	63346,33	31,04	31,04	7,70	73,2
10	11	42747,33	20,95	20,95	5,20	78,4
11	12	36013,33	17,65	17,65	4,38	82,7
12	13	31745,67	15,55	15,55	3,86	86,6
13	14	24659,00	12,08	12,08	3,00	89,6
14	15	20211,33	9,90	9,90	2,46	92,1
15	16	17600,67	8,62	8,62	2,14	94,2
16	18	32154,67	7,88	15,76	1,96	96,2
18	20	21778,33	5,34	10,67	1,32	97,5
20	22	14631,00	3,58	7,17	0,89	98,4
22	24	9599,00	2,35	4,70	0,58	99,0
24	26	6533,00	1,60	3,20	0,40	99,4
26	28	4133,00	1,01	2,03	0,25	99,6
28	30	2653,00	0,65	1,30	0,16	99,8
30	32	1667,33	0,41	0,82	0,10	99,9
32	35	1642,67	0,27	0,80	0,07	99,9
35	38	818,00	0,13	0,40	0,03	100,0
38	41	355,33	0,06	0,17	0,01	100,0
41	44	187,33	0,03	0,09	0,01	100,0
44	47	77,67	0,01	0,04	0,00	100,0
47	53	79,33	0,01	0,04	0,00	100,0
53	59	25,00	0,00	0,01	0,00	100,0
59	65	6,33	0,00	0,00	0,00	100,0
65	71	1,33	0,00	0,00	0,00	100,0
71	77	0,00	0,00	0,00	0,00	100,0
77	83	0,67	0,00	0,00	0,00	100,0
83	89	0,67	0,00	0,00	0,00	100,0
89	95	0,00	0,00	0,00	0,00	100,0
95						
totaal		870891		427	100,00	

Date : march 18 1992 distribution: SURFACE

period: Run 4

diam. interval

upper-limit (um)	lower-limit (um)	surface um^2/m^3 /um	surface um^2/m^3 interval	surface in %	surface accum. %
1	2	110	110	0,1	0,1
2	3	180	180	0,1	0,2
3	4	861	861	0,6	0,8
4	5	1730	1730	1,1	1,9
5	6	3684	3684	2,4	4,3
6	7	6835	6835	4,5	8,8
7	8	9671	9671	6,4	15,2
8	9	10372	10372	6,8	22,0
9	10	8808	8808	5,8	27,8
10	11	7260	7260	4,8	32,5
11	12	7336	7336	4,8	37,4
12	13	7639	7639	5,0	42,4
13	14	6921	6921	4,5	46,9
14	15	6544	6544	4,3	51,2
15	16	6511	6511	4,3	55,5
16	18	7160	14321	9,4	64,9
18	20	6057	12113	8,0	72,9
20	22	4970	9940	6,5	79,4
22	24	3911	7821	5,1	84,6
24	26	3144	6289	4,1	88,7
26	28	2320	4640	3,1	91,8
28	30	1718	3436	2,3	94,0
30	32	1234	2467	1,6	95,6
32	35	947	2840	1,9	97,5
35	38	559	1678	1,1	98,6
38	41	285	854	0,6	99,2
41	44	174	521	0,3	99,5
44	47	83	248	0,2	99,7
47	53	51	306	0,2	99,9
53	59	20	121	0,1	100,0
59	65	6	38	0,0	100,0
65	71	2	9	0,0	100,0
71	77	0	0	0	100,0
77	83	1	7	0,0	100,0
83	89	1	8	0,0	100,0
89	95	0	0	0	100,0
95					
totaal			1,52E+5	100,00	

Date : march 18 1992 distribution: VOLUME

period: Run 4

diam. interval

lower-limit (um)	upper-limit (um)	volume um^3/m^3 /um	volume um^3/m^3 interval	volume in %	volume accum %	mass(*) mg/m^3/ interval
1	2	29	29	0,0	0,0	0,03
2	3	77	77	0,0	0,0	0,08
3	4	509	509	0,1	0,2	0,51
4	5	1308	1308	0,3	0,5	1,31
5	6	3396	3396	0,8	1,3	3,40
6	7	7434	7434	1,8	3,1	7,43
7	8	12124	12124	3,0	6,1	12,12
8	9	14728	14728	3,6	9,7	14,73
9	10	13972	13972	3,4	13,2	13,97
10	11	12724	12724	3,1	16,3	12,72
11	12	14078	14078	3,5	19,8	14,08
12	13	15932	15932	3,9	23,7	15,93
13	14	15586	15586	3,8	27,5	15,59
14	15	15827	15827	3,9	31,4	15,83
15	16	16833	16833	4,1	35,5	16,83
16	18	20335	40669	10,0	45,5	40,67
18	20	19215	38429	9,4	55,0	38,43
20	22	17420	34841	8,6	63,6	34,84
22	24	15010	30020	7,4	70,9	30,02
24	26	13115	26230	6,4	77,4	26,23
26	28	10450	20899	5,1	82,5	20,90
28	30	8310	16620	4,1	86,6	16,62
30	32	6378	12757	3,1	89,8	12,76
32	35	5292	15876	3,9	93,7	15,88
35	38	3407	10222	2,5	96,2	10,22
38	41	1875	5626	1,4	97,6	5,63
41	44	1231	3694	0,9	98,5	3,69
44	47	626	1879	0,5	98,9	1,88
47	53	426	2553	0,6	99,6	2,55
53	59	188	1130	0,3	99,8	1,13
59	65	65	388	0,1	99,9	0,39
65	71	18	108	0,0	100,0	0,11
71	77	0	0	0	100,0	0
77	83	15	88	0,0	100,0	0,09
83	89	18	109	0,0	100,0	0,11
89	95	0	0	0	100,0	0
95						
totaal			4,07E+5	100		407

*) If Rho = 1.0

Date : march 18 1992 distribution: NUMBER

period: Run 5

diam. interval

upper-limit (um)	lower-limit (um)	Raw Counts	aantal n/cc /um	aantal n/cc/ interval	aantal in %	aantal accum. %
1	2	15688,67	7,69	7,69	1,72	1,7
2	3	13787,00	6,76	6,76	1,51	3,2
3	4	33463,67	16,40	16,40	3,67	6,9
4	5	45295,67	22,19	22,19	4,97	11,9
5	6	67682,33	33,16	33,16	7,42	19,3
6	7	94837,33	46,47	46,47	10,40	29,7
7	8	109761,00	53,78	53,78	12,04	41,7
8	9	103688,33	50,80	50,80	11,37	53,1
9	10	81441,67	39,90	39,90	8,93	62,0
10	11	61947,67	30,35	30,35	6,79	68,8
11	12	53652,00	26,29	26,29	5,88	74,7
12	13	47929,33	23,48	23,48	5,26	80,0
13	14	38448,67	18,84	18,84	4,22	84,2
14	15	32204,67	15,78	15,78	3,53	87,7
15	16	27559,33	13,50	13,50	3,02	90,7
16	18	53906,67	13,21	26,41	2,96	93,7
18	20	37425,33	9,17	18,34	2,05	95,8
20	22	25955,00	6,36	12,72	1,42	97,2
22	24	17589,00	4,31	8,62	0,96	98,1
24	26	12415,67	3,04	6,08	0,68	98,8
26	28	8010,67	1,96	3,93	0,44	99,3
28	30	5531,33	1,36	2,71	0,30	99,6
30	32	3596,67	0,88	1,76	0,20	99,8
32	35	3150,67	0,51	1,54	0,12	99,9
35	38	1727,33	0,28	0,85	0,06	99,9
38	41	881,00	0,14	0,43	0,03	100,0
41	44	470,33	0,08	0,23	0,02	100,0
44	47	238,67	0,04	0,12	0,01	100,0
47	53	165,33	0,01	0,08	0,00	100,0
53	59	56,33	0,00	0,03	0,00	100,0
59	65	27,33	0,00	0,01	0,00	100,0
65	71	8,67	0,00	0,00	0,00	100,0
71	77	2,00	0,00	0,00	0,00	100,0
77	83	1,33	0,00	0,00	0,00	100,0
83	89	1,33	0,00	0,00	0,00	100,0
89	95	0,67	0,00	0,00	0,00	100,0
95						
totaal		998549		490	100,00	

Date : march 18 1992 distribution: SURFACE

period: Run 5

diam. interval

upper-limit (um)	lower-limit (um)	surface um^2/m^3 /um	surface um^2/m^3 interval	surface in %	surface accum. %
1	2	56	56	0,0	0,0
2	3	134	134	0,1	0,1
3	4	635	635	0,3	0,4
4	5	1418	1418	0,6	1,0
5	6	3160	3160	1,4	2,3
6	7	6180	6180	2,7	5,0
7	8	9518	9518	4,1	9,1
8	9	11545	11545	5,0	14,0
9	10	11325	11325	4,9	18,9
10	11	10521	10521	4,5	23,4
11	12	10929	10929	4,7	28,1
12	13	11534	11534	5,0	33,0
13	14	10791	10791	4,6	37,7
14	15	10427	10427	4,5	42,1
15	16	10195	10195	4,4	46,5
16	18	12004	24009	10,3	56,8
18	20	10408	20816	8,9	65,8
20	22	8816	17632	7,6	73,3
22	24	7166	14332	6,2	79,5
24	26	5976	11951	5,1	84,6
26	28	4497	8993	3,9	88,5
28	30	3582	7163	3,1	91,5
30	32	2661	5322	2,3	93,8
32	35	1815	5446	2,3	96,2
35	38	1181	3544	1,5	97,7
38	41	706	2117	0,9	98,6
41	44	436	1308	0,6	99,2
44	47	254	761	0,3	99,5
47	53	106	637	0,3	99,8
53	59	45	272	0,1	99,9
59	65	27	162	0,1	100,0
65	71	10	62	0,0	100,0
71	77	3	17	0,0	100,0
77	83	2	13	0,0	100,0
83	89	3	15	0,0	100,0
89	95	1	9	0,0	100,0
95					
totaal			2,33E+5	100,00	

Date : march 18 1992 distribution: VOLUME

period: Run 5

diam. interval

lower-limit (um)	upper-limit (um)	volume um^3/m^3 /um	volume um^3/m^3 interval	volume in %	volume accum %	mass(*) mg/m^3/ interval
1	2	15	15	0,0	0,0	0,02
2	3	57	57	0,0	0,0	0,06
3	4	376	376	0,1	0,1	0,38
4	5	1072	1072	0,2	0,2	1,07
5	6	2913	2913	0,4	0,6	2,91
6	7	6721	6721	1,0	1,6	6,72
7	8	11933	11933	1,7	3,3	11,93
8	9	16393	16393	2,4	5,7	16,39
9	10	17964	17964	2,6	8,3	17,96
10	11	18440	18440	2,7	11,0	18,44
11	12	20974	20974	3,0	14,0	20,97
12	13	24055	24055	3,5	17,5	24,05
13	14	24303	24303	3,5	21,0	24,30
14	15	25218	25218	3,6	24,6	25,22
15	16	26357	26357	3,8	28,4	26,36
16	18	34091	68181	9,8	38,3	68,18
18	20	33020	66039	9,5	47,8	66,04
20	22	30903	61807	8,9	56,7	61,81
22	24	27504	55007	7,9	64,7	55,01
24	26	24925	49849	7,2	71,9	49,85
26	28	20253	40507	5,9	77,7	40,51
28	30	17325	34651	5,0	82,7	34,65
30	32	13759	27518	4,0	86,7	27,52
32	35	10150	30450	4,4	91,1	30,45
35	38	7195	21585	3,1	94,2	21,59
38	41	4650	13950	2,0	96,2	13,95
41	44	3091	9274	1,3	97,6	9,27
44	47	1925	5774	0,8	98,4	5,77
47	53	887	5321	0,8	99,2	5,32
53	59	424	2545	0,4	99,6	2,55
59	65	279	1675	0,2	99,8	1,68
65	71	117	700	0,1	99,9	0,70
71	77	35	208	0,0	99,9	0,21
77	83	29	175	0,0	99,9	0,18
83	89	36	218	0,0	100,0	0,22
89	95	22	133	0,0	100,0	0,13
95						
totaal			6,92E+5	100,00		692

*) If Rho = 1.0

Date : march 18 1992 distribution: NUMBER

period: Run 6

diam. interval

upper-limit (um)	lower-limit (um)	Raw Counts	aantal n/cc /um	aantal n/cc/ interval	aantal in %	aantal accum. %
1	2	16611,40	12,21	12,21	5,25	5,3
2	3	8226,00	6,05	6,05	2,60	7,9
3	4	20625,40	15,16	15,16	6,52	14,4
4	5	23328,40	17,15	17,15	7,38	21,8
5	6	32693,20	24,03	24,03	10,34	32,1
6	7	41873,80	30,78	30,78	13,24	45,3
7	8	41054,00	30,17	30,17	12,98	58,3
8	9	31514,40	23,16	23,16	9,96	68,3
9	10	18988,20	13,96	13,96	6,00	74,3
10	11	12454,00	9,15	9,15	3,94	78,2
11	12	11134,40	8,18	8,18	3,52	81,7
12	13	10127,00	7,44	7,44	3,20	84,9
13	14	8106,80	5,96	5,96	2,56	87,5
14	15	7040,20	5,17	5,17	2,23	89,7
15	16	6442,40	4,73	4,73	2,04	91,8
16	18	12153,80	4,47	8,93	1,92	93,7
18	20	9233,80	3,39	6,79	1,46	95,1
20	22	7221,00	2,65	5,31	1,14	96,3
22	24	5547,60	2,04	4,08	0,88	97,2
24	26	4579,20	1,68	3,37	0,72	97,9
26	28	3477,20	1,28	2,56	0,55	98,4
28	30	2792,60	1,03	2,05	0,44	98,9
30	32	2225,40	0,82	1,64	0,35	99,2
32	35	2517,40	0,62	1,85	0,27	99,5
35	38	1795,80	0,44	1,32	0,19	99,7
38	41	1161,40	0,28	0,85	0,12	99,8
41	44	771,40	0,19	0,57	0,08	99,9
44	47	531,80	0,13	0,39	0,06	99,9
47	53	597,60	0,07	0,44	0,03	100,0
53	59	253,20	0,03	0,19	0,01	100,0
59	65	123,40	0,02	0,09	0,01	100,0
65	71	57,60	0,01	0,04	0,00	100,0
71	77	27,40	0,00	0,02	0,00	100,0
77	83	11,00	0,00	0,01	0,00	100,0
83	89	4,40	0,00	0,00	0,00	100,0
89	95	2,80	0,00	0,00	0,00	100,0
95						
totaal		345305		249	100,00	

Date : march 18 1992 distribution: SURFACE

period: Run 6

diam. interval

upper-limit (um)	lower-limit (um)	surface um^2/m^3 /um	surface um^2/m^3 interval	surface in %	surface accum. %
1	2	89	89	0,1	0,1
2	3	120	120	0,1	0,2
3	4	587	587	0,5	0,6
4	5	1095	1095	0,9	1,5
5	6	2290	2290	1,8	3,3
6	7	4093	4093	3,3	6,6
7	8	5340	5340	4,2	10,8
8	9	5263	5263	4,2	15,0
9	10	3960	3960	3,1	18,1
10	11	3173	3173	2,5	20,7
11	12	3402	3402	2,7	23,4
12	13	3656	3656	2,9	26,3
13	14	3413	3413	2,7	29,0
14	15	3419	3419	2,7	31,7
15	16	3575	3575	2,8	34,5
16	18	4060	8119	6,4	41,0
18	20	3852	7704	6,1	47,1
20	22	3679	7358	5,8	52,9
22	24	3390	6780	5,4	58,3
24	26	3306	6612	5,3	63,6
26	28	2928	5856	4,7	68,2
28	30	2712	5425	4,3	72,5
30	32	2470	4940	3,9	76,5
32	35	2176	6528	5,2	81,6
35	38	1842	5527	4,4	86,0
38	41	1395	4186	3,3	89,4
41	44	1073	3219	2,6	91,9
44	47	848	2543	2,0	93,9
47	53	576	3454	2,7	96,7
53	59	306	1835	1,5	98,1
59	65	183	1096	0,9	99,0
65	71	103	615	0,5	99,5
71	77	58	347	0,3	99,8
77	83	27	163	0,1	99,9
83	89	13	75	0,1	100,0
89	95	9	55	0,0	100,0
95					
totaal			1,26E+5	100,00	

Date : march 18 1992 distribution: VOLUME

period: Run 6

diam. interval

lower-limit (um)	upper-limit (um)	volume um^3/m^3 /um	volume um^3/m^3 interval	volume in %	volume accum %	mass(*) mg/m^3/ interval
1	2	24	24	0,0	0,0	0,02
2	3	51	51	0,0	0,0	0,05
3	4	347	347	0,1	0,1	0,35
4	5	828	828	0,2	0,3	0,83
5	6	2111	2111	0,4	0,7	2,11
6	7	4452	4452	0,9	1,6	4,45
7	8	6695	6695	1,4	3,0	6,69
8	9	7474	7474	1,5	4,5	7,47
9	10	6282	6282	1,3	5,8	6,28
10	11	5561	5561	1,1	6,9	5,56
11	12	6529	6529	1,3	8,2	6,53
12	13	7624	7624	1,6	9,8	7,62
13	14	7686	7686	1,6	11,3	7,69
14	15	8269	8269	1,7	13,0	8,27
15	16	9242	9242	1,9	14,9	9,24
16	18	11529	23058	4,7	19,6	23,06
18	20	12220	24440	5,0	24,6	24,44
20	22	12897	25793	5,3	29,8	25,79
22	24	13012	26024	5,3	35,1	26,02
24	26	13789	27578	5,6	40,8	27,58
26	28	13187	26374	5,4	46,1	26,37
28	30	13121	26241	5,3	51,5	26,24
30	32	12770	25539	5,2	56,7	25,54
32	35	12165	36494	7,4	64,1	36,49
35	38	11221	33662	6,9	71,0	33,66
38	41	9195	27584	5,6	76,6	27,58
41	44	7606	22817	4,6	81,3	22,82
44	47	6433	19298	3,9	85,2	19,30
47	53	4808	28850	5,9	91,1	28,85
53	59	2860	17161	3,5	94,6	17,16
59	65	1891	11344	2,3	96,9	11,34
65	71	1164	6983	1,4	98,3	6,98
71	77	713	4280	0,9	99,2	4,28
77	83	362	2170	0,4	99,6	2,17
83	89	180	1078	0,2	99,8	1,08
89	95	140	840	0,2	100,0	0.84
95						
totaal			4,91E+5	100		491

*) If Rho = 1.0

Date : march 18 1992 distribution: NUMBER

period: Run 7

diam. interval

upper-limit (um)	lower-limit (um)	Raw Counts	aantal n/cc /um	aantal n/cc/ interval	aantal in %	aantal accum. %	std de (n=8) %
1	2	10567,88	8,63	8,63	6,80	6,8	0,50
2	3	4233,75	3,46	3,46	2,72	9,5	0,26
3	4	10666,00	8,71	8,71	6,86	16,4	0,43
4	5	11371,63	9,29	9,29	7,32	23,7	0,44
5	6	15912,50	12,99	12,99	10,24	33,9	0,40
6	7	20246,88	16,53	16,53	13,03	47,0	0,46
7	8	19796,75	16,17	16,17	12,74	59,7	1,05
8	9	14793,88	12,08	12,08	9,52	69,2	0,58
9	10	8601,00	7,02	7,02	5,53	74,8	0,41
10	11	5541,75	4,53	4,53	3,57	78,3	0,39
11	12	5194,00	4,24	4,24	3,34	81,7	0,43
12	13	4871,88	3,98	3,98	3,13	84,8	0,27
13	14	3922,50	3,20	3,20	2,52	87,3	0,34
14	15	3507,88	2,86	2,86	2,26	89,6	0,54
15	16	3125,50	2,55	2,55	2,01	91,6	0,31
16	18	5959,00	2,43	4,87	1,92	93,5	0,59
18	20	4524,13	1,85	3,69	1,46	95,0	0,69
20	22	3574,00	1,46	2,92	1,15	96,1	0,38
22	24	2773,88	1,13	2,27	0,89	97,0	0,42
24	26	2342,63	0,96	1,91	0,75	97,8	0,37
26	28	1797,25	0,73	1,47	0,58	98,3	0,46
28	30	1453,25	0,59	1,19	0,47	98,8	0,27
30	32	1163,50	0,48	0,95	0,37	99,2	0,38
32	35	1327,25	0,36	1,08	0,28	99,5	0,30
35	38	952,63	0,26	0,78	0,20	99,7	0,32
38	41	611,38	0,17	0,50	0,13	99,8	0,19
41	44	412,75	0,11	0,34	0,09	99,9	0,20
44	47	276,13	0,08	0,23	0,06	99,9	0,14
47	53	298,38	0,04	0,24	0,03	100,0	0,16
53	59	138,88	0,02	0,11	0,01	100,0	0,09
59	65	62,88	0,01	0,05	0,01	100,0	0,06
65	71	38,38	0,01	0,03	0,00	100,0	0,05
71	77	16,63	0,00	0,01	0,00	100,0	0,05
77	83	7,88	0,00	0,01	0,00	100,0	0,02
83	89	3,75	0,00	0,00	0,00	100,0	0,04
89	95	2,13	0,00	0,00	0,00	100,0	0,01
95							
totaal		170090		139	100,00		

Date : march 18 1992 distribution: SURFACE

period: Run 7

diam. interval

upper-limit (um)	lower-limit (um)	surface um^2/m^3 /um	surface um^2/m^3 interval	surface in %	surface accum. %
1	2	63	63	0,1	0,1
2	3	69	69	0,1	0,2
3	4	337	337	0,5	0,7
4	5	593	593	0,8	1,5
5	6	1238	1238	1,8	3,3
6	7	2199	2199	3,1	6,4
7	8	2861	2861	4,1	10,5
8	9	2745	2745	3,9	14,4
9	10	1993	1993	2,8	17,3
10	11	1569	1569	2,2	19,5
11	12	1763	1763	2,5	22,0
12	13	1954	1954	2,8	24,8
13	14	1835	1835	2,6	27,4
14	15	1893	1893	2,7	30,1
15	16	1927	1927	2,7	32,9
16	18	2212	4423	6,3	39,2
18	20	2097	4194	6,0	45,2
20	22	2023	4047	5,8	50,9
22	24	1883	3767	5,4	56,3
24	26	1879	3758	5,4	61,7
26	28	1681	3363	4,8	66,5
28	30	1568	3137	4,5	70,9
30	32	1435	2870	4,1	75,0
32	35	1275	3824	5,5	80,5
35	38	1086	3258	4,6	85,1
38	41	816	2448	3,5	88,6
41	44	638	1913	2,7	91,4
44	47	489	1467	2,1	93,5
47	53	319	1916	2,7	96,2
53	59	186	1118	1,6	97,8
59	65	103	621	0,9	98,7
65	71	76	456	0,6	99,3
71	77	39	234	0,3	99,6
77	83	22	129	0,2	99,8
83	89	12	71	0,1	99,9
89	95	8	46	0,1	100,0
95					
totaal			7,01E+4	100,00	

Date : march 18 1992 distribution: VOLUME

period: Run 7

diam. interval

lower-limit (um)	upper-limit (um)	volume um^3/m^3 /um	volume um^3/m^3 interval	volume in %	volume accum %	mass(*) mg/m^3/ interval
1	2	17	17	0,0	0,0	0,02
2	3	29	29	0,0	0,0	0,03
3	4	200	200	0,1	0,1	0,20
4	5	449	449	0,2	0,2	0,45
5	6	1141	1141	0,4	0,7	1,14
6	7	2392	2392	0,9	1,5	2,39
7	8	3587	3587	1,3	2,8	3,59
8	9	3898	3898	1,4	4,2	3,90
9	10	3162	3162	1,1	5,3	3,16
10	11	2749	2749	1,0	6,3	2,75
11	12	3384	3384	1,2	7,5	3,38
12	13	4075	4075	1,5	8,9	4,08
13	14	4132	4132	1,5	10,4	4,13
14	15	4578	4578	1,6	12,0	4,58
15	16	4982	4982	1,8	13,8	4,98
16	18	6281	12562	4,5	18,3	12,56
18	20	6653	13305	4,7	23,0	13,31
20	22	7092	14185	5,1	28,1	14,18
22	24	7229	14458	5,2	33,2	14,46
24	26	7838	15676	5,6	38,8	15,68
26	28	7573	15147	5,4	44,2	15,15
28	30	7587	15173	5,4	49,6	15,17
30	32	7418	14836	5,3	54,9	14,84
32	35	7126	21379	7,6	62,6	21,38
35	38	6614	19841	7,1	69,6	19,84
38	41	5378	16134	5,8	75,4	16,13
41	44	4522	13565	4,8	80,2	13,56
44	47	3711	11134	4,0	84,2	11,13
47	53	2668	16005	5,7	89,9	16,01
53	59	1743	10458	3,7	93,6	10,46
59	65	1070	6422	2,3	95,9	6,42
65	71	862	5169	1,8	97,7	5,17
71	77	481	2885	1,0	98,8	0,23
77	83	288	1726	0,6	99,4	1,73
83	89	170	1021	0,4	99,7	1,02
89	95	118	708	0,3	100,0	0,05
95						
totaal			2,81E+5	100		281

*) If Rho = 1.0

Date : march 18 1992 distribution: NUMBER

period: Run 8

diam. interval

upper-limit (um)	lower-limit (um)	Raw Counts	aantal n/cc /um	aantal n/cc/ interval	aantal in %	aantal accum. %
1	2	3411,75	2,79	2,79	0,68	0,7
2	3	4517,75	3,69	3,69	0,90	1,6
3	4	11356,75	9,27	9,27	2,26	3,8
4	5	16690,50	13,63	13,63	3,33	7,2
5	6	26452,00	21,60	21,60	5,27	12,4
6	7	39599,25	32,34	32,34	7,90	20,3
7	8	49151,00	40,14	40,14	9,80	30,1
8	9	51393,75	41,97	41,97	10,25	40,4
9	10	45481,00	37,14	37,14	9,07	49,5
10	11	38358,25	31,32	31,32	7,65	57,1
11	12	34702,75	28,34	28,34	6,92	64,0
12	13	33029,25	26,97	26,97	6,59	70,6
13	14	28019,25	22,88	22,88	5,59	76,2
14	15	24311,50	19,85	19,85	4,85	81,1
15	16	21600,50	17,64	17,64	4,31	85,4
16	18	45377,00	18,53	37,06	4,52	89,9
18	20	32574,25	13,30	26,60	3,25	93,1
20	22	23179,50	9,46	18,93	2,31	95,4
22	24	15656,75	6,39	12,79	1,56	97,0
24	26	11037,75	4,51	9,01	1,10	98,1
26	28	7091,00	2,90	5,79	0,71	98,8
28	30	4756,25	1,94	3,88	0,47	99,3
30	32	3070,00	1,25	2,51	0,31	99,6
32	35	2950,50	0,80	2,41	0,20	99,8
35	38	1601,00	0,44	1,31	0,11	99,9
38	41	795,75	0,22	0,65	0,05	99,9
41	44	425,25	0,12	0,35	0,03	100,0
44	47	209,25	0,06	0,17	0,01	100,0
47	53	181,00	0,02	0,15	0,01	100,0
53	59	49,50	0,01	0,04	0,00	100,0
59	65	15,00	0,00	0,01	0,00	100,0
65	71	7,25	0,00	0,01	0,00	100,0
71	77	1,25	0,00	0,00	0,00	100,0
77	83	1,25	0,00	0,00	0,00	100,0
83	89	0,50	0,00	0,00	0,00	100,0
89	95	0,25	0,00	0,00	0,00	100,0
95						
totaal		577056		471	100,00	

Date : march 18 1992 distribution: SURFACE

period: Run 8

diam. interval

upper-limit (um)	lower-limit (um)	surface um^2/m^3 /um	surface um^2/m^3 interval	surface in %	surface accum. %
1	2	20	20	0,0	0,0
2	3	73	73	0,0	0,0
3	4	359	359	0,1	0,2
4	5	871	871	0,3	0,5
5	6	2059	2059	0,7	1,2
6	7	4301	4301	1,5	2,6
7	8	7103	7103	2,4	5,1
8	9	9537	9537	3,3	8,3
9	10	10540	10540	3,6	11,9
10	11	10858	10858	3,7	15,6
11	12	11782	11782	4,0	19,7
12	13	13247	13247	4,5	24,2
13	14	13107	13107	4,5	28,7
14	15	13119	13119	4,5	33,1
15	16	13318	13318	4,6	37,7
16	18	16841	33683	11,5	49,2
18	20	15098	30196	10,3	59,5
20	22	13122	26245	9,0	68,5
22	24	10631	21262	7,3	75,8
24	26	8854	17708	6,1	81,8
26	28	6634	13268	4,5	86,4
28	30	5133	10266	3,5	89,9
30	32	3786	7572	2,6	92,4
32	35	2834	8501	2,9	95,4
35	38	1825	5475	1,9	97,2
38	41	1062	3187	1,1	98,3
41	44	657	1971	0,7	99,0
44	47	371	1112	0,4	99,4
47	53	194	1162	0,4	99,8
53	59	66	399	0,1	99,9
59	65	25	148	0,1	100,0
65	71	14	86	0,0	100,0
71	77	3	18	0,0	100,0
77	83	3	21	0,0	100,0
83	89	2	9	0,0	100,0
89	95	1	5	0,0	100,0
95					
totaal			2,93E+5	100,00	

Date : march 18 1992 distribution: VOLUME

period: Run 8

diam. interval

lower-limit (um)	upper-limit (um)	volume um^3/m^3 /um	volume um^3/m^3 interval	volume in %	volume accum %	mass(*) mg/m^3/ interval
1	2	5	5	0,0	0,0	0,01
2	3	31	31	0,0	0,0	0,03
3	4	212	212	0,0	0,0	0,21
4	5	658	658	0,1	0,1	0,66
5	6	1897	1897	0,2	0,3	1,90
6	7	4677	4677	0,5	0,8	4,68
7	8	8906	8906	0,9	1,7	8,91
8	9	13542	13542	1,4	3,2	13,54
9	10	16720	16720	1,8	5,0	16,72
10	11	19030	19030	2,0	7,0	19,03
11	12	22610	22610	2,4	9,4	22,61
12	13	27628	27628	2,9	12,3	27,63
13	14	29517	29517	3,1	15,5	29,52
14	15	31729	31729	3,4	18,8	31,73
15	16	34430	34430	3,7	22,5	34,43
16	18	47827	95655	10,2	32,7	95,65
18	20	47899	95799	10,2	42,9	95,80
20	22	45998	91996	9,8	52,7	92,00
22	24	40804	81607	8,7	61,3	81,61
24	26	36931	73861	7,9	69,2	73,86
26	28	29880	59761	6,4	75,6	59,76
28	30	24829	49659	5,3	80,8	49,66
30	32	19573	39147	4,2	85,0	39,15
32	35	15842	47525	5,1	90,1	47,53
35	38	11115	33345	3,5	93,6	33,34
38	41	7000	21000	2,2	95,8	21,00
41	44	4659	13976	1,5	97,3	13,98
44	47	2812	8437	0,9	98,2	8,44
47	53	1618	9709	1,0	99,3	9,71
53	59	621	3728	0,4	99,7	3,73
59	65	255	1532	0,2	99,8	1,53
65	71	163	977	0,1	99,9	0,98
71	77	36	217	0,0	99,9	0,22
77	83	46	274	0,0	100,0	0,27
83	89	23	136	0,0	100,0	0,14
89	95	14	83	0,0	100,0	0,01
95						
totaal			9,40E+5	100		940

*) If Rho = 1.0

Date : march 18 1992 distribution: NUMBER

period: Run 9

diam. interval

upper-limit (um)	lower-limit (um)	Raw Counts	aantal n/cc /um	aantal n/cc/ interval	aantal in %	aantal accum. %
1	2	7527,33	6,15	6,15	3,83	3,8
2	3	4011,33	3,28	3,28	2,04	5,9
3	4	10689,00	8,73	8,73	5,44	11,3
4	5	11835,33	9,67	9,67	6,02	17,3
5	6	17082,00	13,95	13,95	8,69	26,0
6	7	23913,33	19,53	19,53	12,16	38,2
7	8	25055,33	20,46	20,46	12,74	50,9
8	9	19904,67	16,25	16,25	10,12	61,0
9	10	12411,67	10,14	10,14	6,31	67,3
10	11	8000,00	6,53	6,53	4,07	71,4
11	12	7279,33	5,94	5,94	3,70	75,1
12	13	6936,67	5,66	5,66	3,53	78,6
13	14	5791,00	4,73	4,73	2,94	81,6
14	15	5086,33	4,15	4,15	2,59	84,2
15	16	4738,67	3,87	3,87	2,41	86,6
16	18	9348,33	3,82	7,63	2,38	89,0
18	20	7517,33	3,07	6,14	1,91	90,9
20	22	6395,33	2,61	5,22	1,63	92,5
22	24	5222,67	2,13	4,26	1,33	93,8
24	26	4613,00	1,88	3,77	1,17	95,0
26	28	3778,00	1,54	3,09	0,96	96,0
28	30	3406,33	1,39	2,78	0,87	96,8
30	32	3011,67	1,23	2,46	0,77	97,6
32	35	3757,67	1,02	3,07	0,64	98,2
35	38	3090,33	0,84	2,52	0,52	98,7
38	41	2307,67	0,63	1,88	0,39	99,1
41	44	1739,67	0,47	1,42	0,29	99,4
44	47	1328,33	0,36	1,08	0,23	99,7
47	53	1805,00	0,25	1,47	0,15	99,8
53	59	1023,67	0,14	0,84	0,09	99,9
59	65	571,33	0,08	0,47	0,05	99,9
65	71	304,33	0,04	0,25	0,03	100,0
71	77	159,00	0,02	0,13	0,01	100,0
77	83	83,67	0,01	0,07	0,01	100,0
83	89	49,33	0,01	0,04	0,00	100,0
89	95	28,33	0,00	0,02	0,00	100,0
95						
totaal		229803		169	100,00	

Date : march 18 1992 distribution: SURFACE

period: Run 9

diam. interval

upper-limit (um)	lower-limit (um)	surface um^2/m^3 /um	surface um^2/m^3 interval	surface in %	surface accum. %
1	2	45	45	0,0	0,0
2	3	65	65	0,0	0,1
3	4	338	338	0,2	0,3
4	5	617	617	0,4	0,6
5	6	1329	1329	0,8	1,4
6	7	2597	2597	1,5	3,0
7	8	3621	3621	2,1	5,1
8	9	3694	3694	2,2	7,3
9	10	2876	2876	1,7	9,0
10	11	2264	2264	1,3	10,4
11	12	2471	2471	1,5	11,8
12	13	2782	2782	1,7	13,5
13	14	2709	2709	1,6	15,1
14	15	2745	2745	1,6	16,7
15	16	2922	2922	1,7	18,4
16	18	3470	6939	4,1	22,6
18	20	3484	6969	4,1	26,7
20	22	3621	7241	4,3	31,0
22	24	3546	7092	4,2	35,2
24	26	3700	7401	4,4	39,6
26	28	3535	7069	4,2	43,8
28	30	3676	7352	4,4	48,1
30	32	3714	7428	4,4	52,5
32	35	3609	10826	6,4	59,0
35	38	3523	10568	6,3	65,2
38	41	3081	9242	5,5	70,7
41	44	2688	8065	4,8	75,5
44	47	2353	7058	4,2	79,7
47	53	1932	11591	6,9	86,6
53	59	1374	8244	4,9	91,5
59	65	940	5639	3,3	94,8
65	71	602	3613	2,1	96,9
71	77	372	2235	1,3	98,3
77	83	229	1374	0,8	99,1
83	89	156	936	0,6	99,6
89	95	103	615	0,4	100,0
95					
totaal			1,69E+5	100	

Date : march 18 1992 distribution: VOLUME

period: Run 9

diam. interval

lower-limit (um)	upper-limit (um)	volume um^3/m^3 /um	volume um^3/m^3 interval	volume in %	volume accum %	mass(*) mg/m^3/ interval
1	2	12	12	0,0	0,0	0,01
2	3	28	28	0,0	0,0	0,03
3	4	200	200	0,0	0,0	0,20
4	5	467	467	0,1	0,1	0,47
5	6	1225	1225	0,1	0,2	1,23
6	7	2825	2825	0,3	0,5	2,82
7	8	4540	4540	0,5	1,0	4,54
8	9	5245	5245	0,6	1,6	5,24
9	10	4563	4563	0,5	2,1	4,56
10	11	3969	3969	0,4	2,5	3,97
11	12	4743	4743	0,5	3,0	4,74
12	13	5802	5802	0,6	3,6	5,80
13	14	6101	6101	0,7	4,3	6,10
14	15	6638	6638	0,7	5,0	6,64
15	16	7553	7553	0,8	5,8	7,55
16	18	9853	19706	2,1	8,0	19,71
18	20	11054	22108	2,4	10,4	22,11
20	22	12691	25382	2,7	13,1	25,38
22	24	13611	27222	2,9	16,1	27,22
24	26	15434	30869	3,3	19,4	30,87
26	28	15920	31840	3,4	22,8	31,84
28	30	17782	35565	3,9	26,7	35,56
30	32	19202	38403	4,2	30,9	38,40
32	35	20175	60526	6,6	37,4	60,53
35	38	21455	64364	7,0	44,4	64,36
38	41	20300	60899	6,6	51,0	60,90
41	44	19058	57174	6,2	57,2	57,17
44	47	17853	53559	5,8	63,0	53,56
47	53	16137	96821	10,5	73,4	96,82
53	59	12848	77089	8,3	81,8	77,09
59	65	9726	58358	6,3	88,1	58,36
65	71	6833	40996	4,4	92,5	41,00
71	77	4599	27595	3,0	95,5	2,23
77	83	3057	18342	2,0	97,5	18,34
83	89	2239	13433	1,5	99,0	13,43
89	95	1574	9444	1,0	100,0	0,62
95						
totaal			9,24E+5	100,00		924

*) If Rho = 1.0

Date : march 18 1992 distribution: NUMBER

period: Run 10

diam. interval

upper-limit (um)	lower-limit (um)	Raw Counts	aantal n/cc /um	aantal n/cc/ interval	aantal in %	aantal accum. %
1	2	2839,00	2,32	2,32	0,59	0,6
2	3	3920,00	3,20	3,20	0,82	1,4
3	4	10091,00	8,24	8,24	2,10	3,5
4	5	14762,00	12,06	12,06	3,07	6,6
5	6	23304,33	19,03	19,03	4,85	11,4
6	7	35612,33	29,08	29,08	7,41	18,8
7	8	45040,00	36,78	36,78	9,37	28,2
8	9	47451,67	38,75	38,75	9,87	38,1
9	10	42231,00	34,49	34,49	8,78	46,9
10	11	35641,67	29,11	29,11	7,41	54,3
11	12	32852,00	26,83	26,83	6,83	61,1
12	13	31252,00	25,52	25,52	6,50	67,6
13	14	26689,00	21,79	21,79	5,55	73,2
14	15	23607,33	19,28	19,28	4,91	78,1
15	16	20951,00	17,11	17,11	4,36	82,4
16	18	44882,33	18,33	36,65	4,67	87,1
18	20	33604,00	13,72	27,44	3,49	90,6
20	22	24941,67	10,18	20,37	2,59	93,2
22	24	18000,00	7,35	14,70	1,87	95,0
24	26	13728,67	5,61	11,21	1,43	96,5
26	28	9689,00	3,96	7,91	1,01	97,5
28	30	7274,67	2,97	5,94	0,76	98,2
30	32	5456,33	2,23	4,46	0,57	98,8
32	35	5995,33	1,63	4,90	0,42	99,2
35	38	4063,33	1,11	3,32	0,28	99,5
38	41	2630,67	0,72	2,15	0,18	99,7
41	44	1784,67	0,49	1,46	0,12	99,8
44	47	1224,00	0,33	1,00	0,08	99,9
47	53	1491,00	0,20	1,22	0,05	99,9
53	59	758,33	0,10	0,62	0,03	100,0
59	65	397,67	0,05	0,32	0,01	100,0
65	71	194,67	0,03	0,16	0,01	100,0
71	77	103,33	0,01	0,08	0,00	100,0
77	83	54,67	0,01	0,04	0,00	100,0
83	89	20,67	0,00	0,02	0,00	100,0
89	95	12,00	0,00	0,01	0,00	100,0
95						
totaal		572551		468	100,00	

Date : march 18 1992 distribution: SURFACE

period: Run 10

diam. interval

upper-limit (um)	lower-limit (um)	surface um^2/m^3 /um	surface um^2/m^3 interval	surface in %	surface accum. %
1	2	17	17	0,0	0,0
2	3	64	64	0,0	0,0
3	4	319	319	0,1	0,1
4	5	770	770	0,2	0,3
5	6	1814	1814	0,5	0,8
6	7	3868	3868	1,0	1,8
7	8	6509	6509	1,8	3,6
8	9	8806	8806	2,4	6,0
9	10	9787	9787	2,6	8,6
10	11	10089	10089	2,7	11,3
11	12	11153	11153	3,0	14,3
12	13	12534	12534	3,4	17,7
13	14	12485	12485	3,4	21,0
14	15	12739	12739	3,4	24,5
15	16	12918	12918	3,5	27,9
16	18	16658	33316	9,0	36,9
18	20	15576	31151	8,4	45,3
20	22	14120	28240	7,6	52,9
22	24	12222	24444	6,6	59,5
24	26	11012	22025	5,9	65,4
26	28	9065	18129	4,9	70,3
28	30	7851	15702	4,2	74,5
30	32	6729	13457	3,6	78,1
32	35	5758	17273	4,6	82,7
35	38	4632	13896	3,7	86,5
38	41	3512	10535	2,8	89,3
41	44	2758	8274	2,2	91,5
44	47	2168	6503	1,7	93,3
47	53	1596	9574	2,6	95,9
53	59	1018	6107	1,6	97,5
59	65	654	3925	1,1	98,6
65	71	385	2311	0,6	99,2
71	77	242	1452	0,4	99,6
77	83	150	898	0,2	99,8
83	89	65	392	0,1	99,9
89	95	43	261	0,1	100,0
95					
totaal			3,72E+5	100,00	

Date : march 18 1992 distribution: VOLUME

period: Run 10

diam. interval

lower-limit (um)	upper-limit (um)	volume um^3/m^3 /um	volume um^3/m^3 interval	volume in %	volume accum %	mass(*) mg/m^3/ interval
1	2	5	5	0,0	0,0	0,00
2	3	27	27	0,0	0,0	0,03
3	4	189	189	0,0	0,0	0,19
4	5	582	582	0,0	0,1	0,58
5	6	1672	1672	0,1	0,2	1,67
6	7	4207	4207	0,3	0,4	4,21
7	8	8161	8161	0,5	1,0	8,16
8	9	12503	12503	0,8	1,8	12,50
9	10	15525	15525	1,0	2,8	15,52
10	11	17682	17682	1,2	4,0	17,68
11	12	21404	21404	1,4	5,4	21,40
12	13	26141	26141	1,7	7,2	26,14
13	14	28116	28116	1,9	9,0	28,12
14	15	30810	30810	2,0	11,1	30,81
15	16	33394	33394	2,2	13,3	33,39
16	18	47306	94612	6,3	19,6	94,61
18	20	49414	98827	6,6	26,1	98,83
20	22	49495	98990	6,6	32,7	98,99
22	24	46910	93821	6,2	38,9	93,82
24	26	45934	91868	6,1	45,0	91,87
26	28	40828	81656	5,4	50,4	81,66
28	30	37977	75953	5,0	55,5	75,95
30	32	34788	69576	4,6	60,1	69,58
32	35	32190	96570	6,4	66,5	96,57
35	38	28210	84629	5,6	72,1	84,63
38	41	23141	69423	4,6	76,7	69,42
41	44	19551	58653	3,9	80,6	58,65
44	47	16451	49353	3,3	83,9	49,35
47	53	13330	79978	5,3	89,2	79,98
53	59	9518	57107	3,8	92,9	57,11
59	65	6770	40619	2,7	95,6	40,62
65	71	4371	26223	1,7	97,4	26,22
71	77	2989	17934	1,2	98,6	17.93
77	83	1997	11985	0,8	99,4	11,98
83	89	938	5628	0,4	99,7	5,63
89	95	667	4000	0,3	100,0	4,00
95						
totaal			1,51E+6	100,00		1510

*) If Rho = 1.0

APPENDIX D

ASTEX C-131A FLIGHTS
CLOUD MICROPHYSICS PROBE (PVM-100A)
DATA: ~10 HZ, 1 HZ; ASCII; DOS COMPATIBLE
1) LWC (LIQUID WATER CONTENT; G/M^3)
2) PSA (PARTICLE SURFACE AREA; CM^2/M^3)
3) R(EFF) (EFFECTIVE DROPLET RADIUS, UM)

(H. GERBER; 1643 BENTANA WAY, RESTON, VA 22090)
(PHONE 703-742-9844; FAX 703-742-3374)

FLIGHT NO.	INTERVAL NO.	U. OF WASH. TIME INTERVAL (hhmmss - hhmmss)	10 HZ DATA FILE	1 HZ DATA FILE
1557	1	092900 - 100300	ASTEX01.10	ASTEX01.1HZ
(2 June)	2	101000 - 105656.1	ASTEX02.10	ASTEX02.1HZ
	3	112600 - 122000	ASTEX03.10	ASTEX03.1HZ
1558	4	110500 - 115700	ASTEX04.10	ASTEX04.1HZ
(4 June)	5	123100 - 133300	ASTEX05.10	ASTEX05.1HZ
	6	140800 - 145200	ASTEX06.10	ASTEX06.1HZ
1559	7	104333 - 104800	ASTEX07.10	ASTEX07.1HZ
(8 June)	8	115000 - 125600	ASTEX08.10	ASTEX08.1HZ
1560		NO CLOUDS		
(10 June)				
1561	9	093600 - 101100	ASTEX09.10	ASTEX09.1HZ
(12 June)	10	102200 - 111200	ASTEX10.10	ASTEX10.1HZ
	11	113500 - 121800	ASTEX11.10	ASTEX11.1HZ
	12	131300 - 134500	ASTEX12.10	ASTEX12.1HZ
	13	142100 - 144000	ASTEX13.10	ASTEX13.1HZ
1562	15	100900 - 101600	ASTEX15.10	ASTEX15.1HZ
(13 June)	16	110000 - 111000	ASTEX16.10	ASTEX16.1HZ
	17	114300 - 114900	ASTEX17.10	ASTEX17.1HZ
	18	125700 - 135800	ASTEX18.10	ASTEX18.1HZ
	19	140100 - 144900	ASTEX19.10	ASTEX19.1HZ
1563	20	151200 - 160500	ASTEX20.10	ASTEX20.1HZ
(15 June)	21	161100 - 165000	ASTEX21.10	ASTEX21.1HZ
1564	22	115500 - 122500	ASTEX22.10	ASTEX22.1HZ
(16 June)	23	150500 - 154000	ASTEX23.10	ASTEX23.1HZ
1565	24	091000 - 091500	ASTEX24.10	ASTEX24.1HZ
(17 June)	25	093700 - 103700	ASTEX25.10	ASTEX25.1HZ

	26	103700 - 113200	ASTEX26.10	ASTEX26.1HZ
	27 (1)	114500 - 123600	ASTEX27.10 ASTEX27.1	ASTEX27.1HZ
	28	125800 - 130100	ASTEX28.10	ASTEX28.1HZ
1566 (19 June)		NO CLOUDS		
1567	29	161500 - 161800	ASTEX29.10	ASTEX29.1HZ
(20 June)	31	200200 - 201200	ASTEX31.10	ASTEX31.1HZ
1568	32	090100 - 090600	ASTEX32.10	ASTEX32.1HZ
(21 June)	33	093800 - 103800	ASTEX33.10	ASTEX33.1HZ
	34	103800 - 110000	ASTEX34.10	ASTEX34.1HZ
	35	111600 - 112900	ASTEX35.10	ASTEX35.1HZ
1569	36	050800 - 051100	ASTEX36.10	ASTEX36.1HZ
(22 June)	37	053100 - 053300	ASTEX37.10	ASTEX37.1HZ
	38	055300 - 061100	ASTEX38.10	ASTEX38.1HZ
	39	070800 - 071100	ASTEX39.10	ASTEX39.1HZ
	40	072600 - 073000	ASTEX40.10	ASTEX40.1HZ
	41	081000 - 090600	ASTEX41.10	ASTEX41.1HZ
1570 (23 June)	42	131500 - 135000	ASTEX42.10	ASTEX42.1HZ
1571	43	094200 - 104000	ASTEX43.10	ASTEX43.1HZ
(26 June)	44	104000 - 114000	ASTEX44.10	ASTEX44.1HZ
	45	114000 - 124000	ASTEX45.10	ASTEX45.1HZ
	46	124100 - 134200	ASTEX46.10	ASTEX46.1HZ
	47	140000 - 150200	ASTEX47.10	ASTEX47.1HZ
1572 (27 June)		NO CLOUDS		

NOTES:

(1) PSA channel inoperative during this interval. R(EFF) estimated by correcting FSSP data; see ASTEX27.1.

(2) Due to digital round-off errors in the raw data, the data rate in the 10 HZ DATA FILES is 9.84572 Hz, except for files 32,36,37,38,39,40,41 where the data rate is 10.03773 Hz, and except for file 33 where the rate is 10.00000 Hz. All the ~10 Hz data has been synchronized with the U. of Washington 1.00000 Hz data files.

DATA REDUCTION

1. Introduction - The raw data of LWC and PSA collected with the PVM-100A on the C-131A flights resides in the U. of Washington ASTEX data base. The following summarizes the reduction of this raw data.

2. Scaling Constants - The following equations relate LWC and PSA to output voltages and scaling constants of the PVM-100A:

LWC (G/M^3) = LWC (VOLTAGE) x 2.580
PSA (CM^2/M^3) = PSA (VOLTAGE) x 7,700

The raw data set consists of LWC and PSA voltages. The reduced data set consist of values to which the scaling constants have been applied. The scaling constants were determined in a calibration as described in "New Microphysics Sensor for Aircraft Use" by Gerber, H., Arends, B.G. and Ackerman, A., 1993; Submitted to Atmospheric Research.

3. Voltage Offsets - The raw voltage data for the LWC and PSA channels contained voltage offsets which were typically -.050 V for each channel. The reduced data has these offsets removed.

4. Calculation of R(EFF) - The equation for R(EFF) is given by

R(EFF) = 30,000 x (LWC/PSA)

Since R(EFF) is proportional to the ratio of LWC/PSA, large errors in R(EFF) will result when LWC and PSA approach zero value. Conditional statements are applied to the LWC and PSA data, which return the relationship R(EFF) = 0 when the values of LWC and PSA are smaller than a specified value:

IF LWC < .020 G/M^3 THEN R(EFF) = 0
IF PSA < 60 CM^2/M^3 THEN R(EFF) = 0

The reduced R(EFF) data contains the effect of these conditional statements.

The reduced R(EFF) data shows single data-point spikes that can occur when there are large changes in the density of the cloud, such as at cloud edge. These spikes are a result of a 26-ms displacement of the A to D conversion between LWC and PSA channels; this displacement corresponds to about a 2-m distance along the C-131A flight path given the 80 m/s speed of the aircraft. Spikes in R(EFF) occur when the PSA measurement occurs out of cloud and the LWC measurement occurs incloud; and spurious 0 values of R(EFF) occur when the measurement sequence of LWC and PSA is reversed with repect to the cloud edge. Spikes and spurious 0 values have not been removed from the reduced data set.

5. ACCURACY - The accuracy of the LWC channel is ~5%, and the precision of the LWC and PSA channels is ~2%, for the droplet-size bandpass of the instrument's design. The accuracy of the PSA channel is estimated to be similar to the accuracy of the LWC channel, because of calibration, and of the physical consistency of the data produced by both channels in this ASTEX data base. However, some doubt must remain as to the accuracy of PSA, since the calibration of this channel depended in part on the performance of a FSSP used during the instrument's calibration in the cloud chamber at ECN, Petten. The instrument's response gradually rolls off for cloud droplets $\lesssim$ 5 um and $\gtrsim$ 50 um; 50% points are ~2 um and ~70 um for LWC.

6. 1 HZ DATA - Each ~10 Hz ASTEX*.10 data file was averaged over ~1-s increments. A 1 Hz data file titled ASTEX*.1HZ was generated from each averaged file. The 1 Hz files contain LWC, PSA, and R(EFF) measured by the PVM. The 1 Hz files also contain LWC, PSA, R(EFF) found by summing the measurements of the PVM and the U. of Washington's OAP-200X drizzle probe that has 15 droplet size channels ranging from 20 um to 320 um. (The ~10 Hz data leads the 1 Hz data by 0.5 s, because the OAP-200X produces an output at the end of its 1-s sampling time.)

Given that the PVM has a gradual roll off in response for larger droplets, requires that only a portion of the output of each channel of the OAP-200X is used when summing with the PVM to determine the 1 Hz data. The estimated response of the PVM as a function of OAP-200X channel droplet diameter is as follows:

OAP-200X		% Measured by PVM-100A	
Channel No.	Droplet Size (um)	LWC Channel	PSA Channel
1	20 - 40	100	100
2	40 - 60	81	100
3	60 - 80	46	88
4	80 - 100	22	55
5	100 - 120	12.3	33
6	120 - 140	8.3	29
7	140 - 160	6.0	26
8	160 - 180	4.2	24
9	180 - 200	3.2	22
10	200 - 220	2	20
11	220 - 240	2	18
12	240 - 260	1	16
13	260 - 280	1	12
14	280 - 300	0	8
15	300 - 320	0	6

"ASTEX21.10"

FLT 1563	June 15	Interval	No. 21
U.W. Time	fr161100	to165000	
time	LWC	PSA	r(eff)
(s)	(g/m^3)	(cm^2/m^3)	(um)
0.000	-0.008	-38.500	0.000
0.102	-0.008	-38.497	0.000
0.203	-0.008	-38.494	0.000
0.305	-0.008	-15.391	0.000
0.406	-0.008	-15.388	0.000
0.508	-0.008	-15.385	0.000
0.609	-0.008	-38.482	0.000
0.711	-0.008	-38.479	0.000
0.813	-0.008	-38.476	0.000
0.914	-0.008	-15.373	0.000
1.016	-0.008	-38.470	0.000
1.117	-0.008	-15.367	0.000
1.219	-0.008	-15.364	0.000
1.320	-0.008	-15.361	0.000
1.422	-0.013	-15.358	0.000
1.524	-0.008	-15.355	0.000
1.625	-0.008	-15.352	0.000
1.727	-0.008	-15.349	0.000
1.828	-0.008	-38.446	0.000
1.930	-0.008	-15.343	0.000
2.031	-0.008	-38.440	0.000

C-2

"ASTEX21.1HZ"

FLT 1563 U.W. Time time (s)	June 15 fr161100 LWC (g/m^3)	Interval to165000 PSA (cm^2/m^3)	No. 21 -- r(eff) (um)	WITH DRIZZLE LWC (g/m^3)	WITH DRIZZLE PSA (cm^2/m^3)	WITH DRIZZLE r(eff) (um)
0.000	0.000	0.000	0.000	0.000	0.000	0.000
1.016	-0.008	-29.243	0.000	-0.008	-29.243	0.000
2.031	-0.009	-19.973	0.000	-0.009	-19.973	0.000
3.047	-0.008	-24.564	0.000	-0.008	-24.564	0.000
4.063	0.009	26.286	0.000	0.009	26.286	0.000
5.078	0.003	10.147	0.000	0.003	10.147	0.000
6.094	0.000	-1.373	0.000	0.000	-1.373	0.000
7.008	0.000	-2.886	0.000	0.000	-2.886	0.000
8.024	-0.001	0.224	0.000	-0.001	0.224	0.000
9.039	-0.002	0.255	0.000	-0.002	0.255	0.000
10.055	0.000	-1.256	0.000	0.000	-1.256	0.000

Report Documentation Page

1. Report No.	2. Government Accession No.	3. Recipient's Catalog No.
N/A		N/A

4. Title and Subtitle

TITLE: TEST OF PROTOTYPE LIQUID-WATER-CONTENT METER FOR AIRCRAFT USE
SUBTITLE: ADDENDIX D: REDUCTION OF PVM-100A DATA ON ASTEX C-131 FLIGHTS.

5. Report Date
MARCH 12, 1993

6. Performing Organization Code
N/A

7. Author(s)
HERMANN E. GERBER

8. Performing Organization Report No.
N/A

10. Work Unit No.

9. Performing Organization Name and Address
GERBER SCIENTIFIC INC.
1643 BENTANA WAY
RESTON, VA 22090

11. Contract or Grant No.
913-44468

13. Type of Report and Period Covered
FINAL

12. Sponsoring Agency Name and Address
NASA GODDARD
GREENBELT, MD 20771

14. Sponsoring Agency Code
900

15. Supplementary Notes

16. Abstract

ALL DATA COLLECTED WITH THE PVM-100A ON THE UNIVERSITY OF WASHINGTON C131A DURING ASTEX FLIGHTS WAS REDUCED. DATA FILES WERE GENERATED USING THE RAW DATA FROM WHICH OFFSETS, CALIBRATION SPIKES, AND DRIFTS WERE REMOVED. INCONSISTENCIES IN THE U. OF WASHINGTON TIME SCALE WERE CORRECTED. THE DATA FILES CONSIST OF 10 HZ AND 1 HZ DATA OF LIQUID WATER CONTENT, PARTICLE SURFACE AREA, AND DROPLET EFFECTIVE RADIUS. DRIZZLE DATA FROM THE U. OF WASHINGTON OAP-200P PROBE WAS COMBINED WITH 1 HZ DATA TO YIELD A SECOND SET OF 1-HZ DATA FILES.

17. Key Words (Suggested by Author(s))	18. Distribution Statement
MARINE STRATOCUMULUS CLOUDS LIQUID WATER CONTENT DROPLET EFFECTIVE RADIUS CLOUD RADIATION PROPERTIES	N/A

19. Security Classif. (of this report)	20. Security Classif. (of this page)	21. No. of pages	22. Price
U	U	97	N/A

NASA Form 1626